

# Theoretical Study on Anisotropic Magnetoresistance Effects of Arbitrary Directions of Current and Magnetization for Ferromagnets: Application to Transverse Anisotropic Magnetoresistance Effect

Satoshi Kokado<sup>1\*</sup> and Masakiyo Tsunoda<sup>2,3</sup>

<sup>1</sup>*Electronics and Materials Science Course, Department of Engineering, Graduate School of Integrated Science and Technology, Shizuoka University, Hamamatsu 432-8561, Japan*

<sup>2</sup>*Department of Electronic Engineering, Graduate School of Engineering, Tohoku University, Sendai 980-8579, Japan*

<sup>3</sup>*Center for Spintronics Research Network, Tohoku University, Sendai 980-8577, Japan*

We develop a theory of the anisotropic magnetoresistance (AMR) effects of arbitrary directions of current and magnetization for ferromagnets. Here, we use the electron scattering theory with the  $s$ - $s$  and  $s$ - $d$  scattering processes, where  $s$  is the conduction electron state and  $d$  is the localized d states. The resistivity due to electron scattering is expressed by the probability density of the d states of the current direction. The d states are numerically obtained by applying the exact diagonalization method to the Hamiltonian of the d states with the exchange field, crystal field, and spin-orbit interaction. Using the theory, we investigate the transverse AMR (TAMR) effect for strong ferromagnets with a crystal field of cubic or tetragonal symmetry. The cubic systems exhibit the fourfold symmetric TAMR effect, whereas the tetragonal systems show the twofold and fourfold symmetric TAMR effect. On the basis of the above results, we also comment on the experimental results of the TAMR effect for Fe<sub>4</sub>N.

## 1. Introduction

The anisotropic magnetoresistance (AMR) effect for ferromagnets is a fundamental phenomenon in which the electrical resistivity depends on the direction of magnetization  $\mathbf{M}$ .<sup>1-20)</sup> Figure 1 shows the sample geometry for the AMR measurement. The current

---

\*E-mail address: kokado.satoshi@shizuoka.ac.jp

$\mathbf{I}$  flows in the direction indexed by  $\Theta$  and  $\Phi$ , where  $\Theta$  and  $\Phi$  are the polar angle and azimuthal angle of  $\mathbf{I}$ , respectively. The thermal average of the spin  $\langle \mathbf{S} \rangle$  ( $\propto -\mathbf{M}$ ) is oriented in the direction indexed by  $\theta$  and  $\phi$ , where  $\theta$  and  $\phi$  are the polar angle and azimuthal angle of  $\langle \mathbf{S} \rangle$ , respectively. The efficiency of the effect, the ‘‘AMR ratio’’, is defined by

$$\text{AMR}(\Theta, \Phi; \theta, \phi) = \frac{\rho(\Theta, \Phi; \theta, \phi) - \rho(\Theta, \Phi; \theta_0, \phi_0)}{\rho(\Theta, \Phi; \theta_0, \phi_0)}. \quad (1)$$

Here,  $\rho(\Theta, \Phi; \theta, \phi)$  represents resistivity at  $(\Theta, \Phi)$  and  $(\theta, \phi)$ , as will be given by Eq. (18). In addition,  $\theta_0$  and  $\phi_0$  are the specific  $\theta$  and  $\phi$ , which are chosen as the reference direction.

Usually, the AMR ratio is experimentally measured for the in-plane configuration, in which  $\mathbf{I}$  flows in the [100] or [110] direction and  $\mathbf{M}$  lies in the (001) plane.<sup>6,7,19,20</sup> In addition, the in-plane AMR ratios have often been analyzed by using analytic expressions of the AMR ratio derived from the electron scattering theory.<sup>12–17</sup> This theory has taken into account all the electron scattering processes from the conduction state to the localized d states through a nonmagnetic impurity. The wave functions of the d states have been analytically obtained within the perturbation theory.

Currently, AMR effects are being investigated for various directions of  $\mathbf{I}$  and  $\mathbf{M}$ . For example, Kabara *et al.*<sup>21,22</sup> experimentally observed the transverse AMR (TAMR) effect for Fe<sub>4</sub>N, where Fe<sub>4</sub>N is considered to be a strong ferromagnet.<sup>12,14,23</sup> In this effect,  $\mathbf{I}$  flows in the [100] direction (i.e.,  $\Theta = \pi/2$  and  $\Phi = 0$ ) and  $\mathbf{M}$  lies in the (100) plane (i.e., an arbitrary  $\theta$  and  $\phi = \pi/2$ ). The TAMR ratio is defined by

$$\text{TAMR}(\theta) = \frac{\rho(\theta) - \rho(0)}{\rho(0)}, \quad (2)$$

with  $\rho(\theta) = \rho(\pi/2, 0; \theta, \pi/2)$ , where  $\theta = 0$  is chosen as the reference direction. This TAMR( $\theta$ ) of Eq. (2) is generally expressed as

$$\text{TAMR}(\theta) = C_0 + C_2 \cos 2\theta + C_4 \cos 4\theta, \quad (3)$$

where  $C_0$  is a constant term and  $C_2$  ( $C_4$ ) is the coefficient of the twofold (fourfold) symmetric term. They reported that Fe<sub>4</sub>N exhibits the enhancement of  $|C_2|$  and  $|C_4|$  for  $T \lesssim 35$  K, i.e., a change from the fourfold symmetric TAMR( $\theta$ ) with  $C_2 = 0$  and  $C_4 = -0.005$  at  $T \sim 35$  K to the twofold and fourfold symmetric TAMR( $\theta$ ) with  $C_2 = -0.02$  and  $C_4 = -0.01$  at  $T = 5$  K.<sup>21,22</sup> In addition, using the multi-orbital d-impurity Anderson model, Yahagi *et al.*<sup>24</sup> confirmed that the system with the crystal field of cubic symmetry shows the fourfold symmetric TAMR( $\theta$ ) with  $C_2 = 0$  and  $C_4 \neq 0$ . Such

a TAMR effect has also been measured to separate the contributions from the TAMR effect and the spin Hall magnetoresistance effect in the whole magnetoresistance effect for a nonmagnet/ferrimagnet structure,<sup>25)</sup> for example.

In the future, AMR effects will be examined more extensively for various directions of  $\mathbf{I}$  and  $\mathbf{M}$ . On the other hand, theories to systematically investigate various AMR effects have seldom been proposed. In particular, the twofold and fourfold TAMR effect has rarely been investigated theoretically. We also note that it may be difficult to obtain an analytic expression of the AMR ratio of arbitrary directions of  $\mathbf{I}$  and  $\mathbf{M}$  or TAMR( $\theta$ ) by the perturbation theory.

In this paper, we first develop a theory of the AMR effects of arbitrary directions of  $\mathbf{I}$  and  $\mathbf{M}$  for ferromagnets by taking into account all the electron scattering processes from the conduction state to the localized d states. The wave functions of the d states are numerically obtained by using the exact diagonalization method for the Hamiltonian of the d states with the exchange field, crystal field, and spin-orbit interaction. Using this theory, we next investigate the TAMR effect for strong ferromagnets. We find that the system with the crystal field of cubic symmetry exhibits the fourfold symmetric TAMR effect, while the system with the crystal field of tetragonal symmetry shows the twofold and fourfold symmetric TAMR effect. Finally, on the basis of the above results, we comment on the experimental results of the TAMR effect for Fe<sub>4</sub>N.

The present paper is organized as follows. In Sect. 2, we describe a theory of the AMR effects of arbitrary directions of  $\mathbf{I}$  and  $\mathbf{M}$  for ferromagnets. In Sect. 3, we apply the theory to the TAMR effects. In Sect. 4, we investigate the TAMR effects for strong ferromagnets with a crystal field of cubic or tetragonal symmetry. In Sect. 5, we comment on the experimental results of the TAMR effect for Fe<sub>4</sub>N. The conclusion is presented in Sect. 6. In Appendix , we show the relation between TAMR( $\theta$ ) and the probability density of the d states of the  $\mathbf{I}$  direction for strong ferromagnets. Appendix gives the approximate expression of TAMR( $\theta$ ) for strong ferromagnets. In Appendix , we approximately obtain the condition for the probability density of the d states of the  $\mathbf{I}$  direction.

## 2. Theory

In this section, we describe the electron scattering theory to obtain  $\rho(\Theta, \Phi; \theta, \phi)$  for ferromagnets. This theory is developed on the basis of our previous study.<sup>12-17)</sup> Here, we use the two-current model with the  $s$ - $s$  and  $s$ - $d$  scatterings for the system shown in

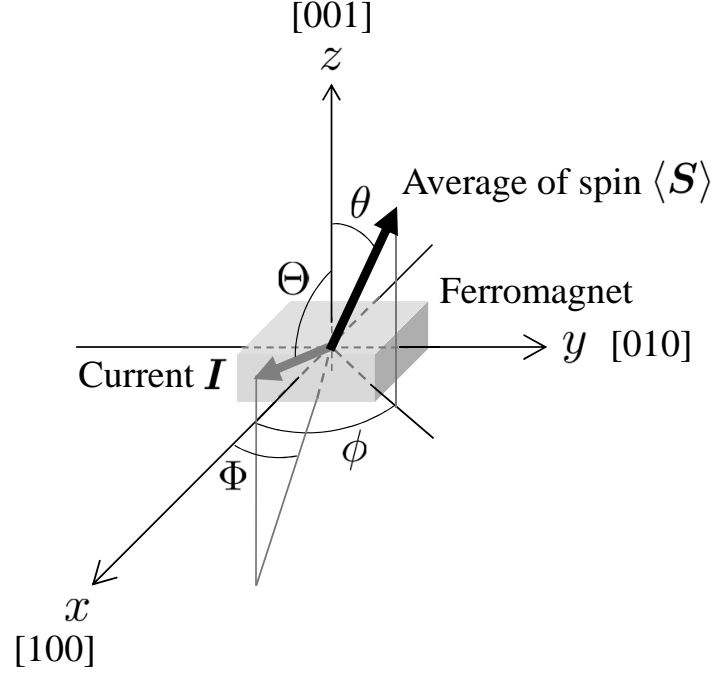


**Fig. 1.** Sketch of sample geometry for AMR measurement. The current  $\mathbf{I}$  flows in the direction indexed by  $\Theta$  and  $\Phi$ , which are the polar angle and azimuthal angle of  $\mathbf{I}$ , respectively. The thermal average of the spin  $\langle \mathbf{S} \rangle$  ( $\propto -\mathbf{M}$ ) is oriented in the direction indexed by  $\theta$  and  $\phi$ , which are the polar angle and azimuthal angle of  $\langle \mathbf{S} \rangle$ , respectively. In addition, the  $x$ -,  $y$ -, and  $z$ -axes are specified to describe the Hamiltonian of Eq. (4).

Fig. 1, where  $s$  is the conduction electron state and  $d$  is the localized  $d$  states.<sup>12–17)</sup>

### 2.1 Hamiltonian

To obtain the localized  $d$  states, we give the Hamiltonian  $\mathcal{H}$  of the localized  $d$  states of a single atom in a ferromagnet with orbital energies, an exchange field, and a spin–orbit interaction. The Hamiltonian  $\mathcal{H}$  is expressed as

$$\mathcal{H} = \mathcal{H}_{\text{orbital}} + \mathcal{H}_{\text{ex}} + \mathcal{H}_{\text{so}}, \quad (4)$$

where

$$\begin{aligned} \mathcal{H}_{\text{orbital}} = \sum_{\sigma=+,-} & \left( E_{xy} |xy, \chi_{\sigma}(\theta, \phi)\rangle \langle xy, \chi_{\sigma}(\theta, \phi)| + E_{yz} |yz, \chi_{\sigma}(\theta, \phi)\rangle \langle yz, \chi_{\sigma}(\theta, \phi)| \right. \\ & + E_{xz} |xz, \chi_{\sigma}(\theta, \phi)\rangle \langle xz, \chi_{\sigma}(\theta, \phi)| \\ & + E_{x^2-y^2} |x^2 - y^2, \chi_{\sigma}(\theta, \phi)\rangle \langle x^2 - y^2, \chi_{\sigma}(\theta, \phi)| \\ & \left. + E_{3z^2-r^2} |3z^2 - r^2, \chi_{\sigma}(\theta, \phi)\rangle \langle 3z^2 - r^2, \chi_{\sigma}(\theta, \phi)| \right), \quad (5) \end{aligned}$$

$$\mathcal{H}_{\text{ex}} = -\mathbf{S} \cdot \mathbf{H}, \quad (6)$$

$$\mathcal{H}_{\text{so}} = \lambda(L_x S_x + L_y S_y) + \lambda' L_z S_z, \quad (7)$$

with

$$\mathbf{S} = (S_x, S_y, S_z), \quad (8)$$

$$\mathbf{L} = (L_x, L_y, L_z), \quad (9)$$

$$\mathbf{H} = H (\sin \theta \cos \phi, \sin \theta \sin \phi, \cos \theta). \quad (10)$$

The above terms are explained as follows. The term  $\mathcal{H}_{\text{ex}}$  is the interaction between the spin angular momentum  $\mathbf{S}$  and the exchange field of the ferromagnet  $\mathbf{H}$ , where  $\mathbf{H} \propto -\mathbf{M}$ ,  $\mathbf{H} \propto \langle \mathbf{S} \rangle$ , and  $H > 0$ . The term  $\mathcal{H}_{\text{so}}$  is the spin-orbit interaction, where  $\mathbf{L}$  is the orbital angular momentum,  $\lambda$  is the spin-orbit coupling constant of the  $L_x S_x + L_y S_y$  operator, and  $\lambda'$  is the spin-orbit coupling constant of the  $L_z S_z$  operator. The different symbols  $\lambda$  and  $\lambda'$  are introduced to determine the contributions of the respective terms to the d states, where they are unique in a spherically symmetric potential. The spin quantum number  $S$  and the azimuthal quantum number  $L$  are chosen to be  $S = 1/2$  and  $L = 2$ .<sup>12)</sup> The term  $\mathcal{H}_{\text{orbital}}$  represents the orbital energies. The quantity  $E_i$  is the energy level of the  $i$  orbital, where  $i = xy, yz, xz, x^2 - y^2$ , and  $3z^2 - r^2$ . The state  $|i, \chi_\sigma(\theta, \phi)\rangle$  is expressed by  $|i, \chi_\sigma(\theta, \phi)\rangle = |i\rangle |\chi_\sigma(\theta, \phi)\rangle$ . The state  $|i\rangle$  is the orbital state, defined by  $|xy\rangle = xyf(r)$ ,  $|yz\rangle = yzf(r)$ ,  $|xz\rangle = xzf(r)$ ,  $|x^2 - y^2\rangle = (1/2)(x^2 - y^2)f(r)$ , and  $|3z^2 - r^2\rangle = [1/(2\sqrt{3})](3z^2 - r^2)f(r)$ , with  $r = \sqrt{x^2 + y^2 + z^2}$  and  $f(r) = \Gamma e^{-\zeta r}$ , where  $f(r)$  is the radial part of the d orbital, and  $\Gamma$  and  $\zeta$  are constants. The state  $|\chi_\sigma(\theta, \phi)\rangle$  ( $\sigma = +$  and  $-$ ) is the spin state, i.e.,

$$|\chi_+(\theta, \phi)\rangle = e^{-i\phi} \cos \frac{\theta}{2} |\uparrow\rangle + \sin \frac{\theta}{2} |\downarrow\rangle, \quad (11)$$

$$|\chi_-(\theta, \phi)\rangle = -e^{-i\phi} \sin \frac{\theta}{2} |\uparrow\rangle + \cos \frac{\theta}{2} |\downarrow\rangle, \quad (12)$$

which are eigenstates of  $\mathcal{H}_{\text{ex}}$ . Here,  $|\chi_+(\theta, \phi)\rangle$  ( $|\chi_-(\theta, \phi)\rangle$ ) denotes the up spin state (down spin state) for the case in which the quantization axis is chosen along the  $\langle \mathbf{S} \rangle$  direction. The state  $|\uparrow\rangle$  ( $|\downarrow\rangle$ ) represents the up spin state (down spin state) for the case in which the quantization axis is chosen along the  $z$ -axis. In addition, this system is a normalized orthogonal system with  $\langle i'|i\rangle = \delta_{i',i}$  and  $\langle \chi_{\sigma'}(\theta, \phi) | \chi_\sigma(\theta, \phi) \rangle = \delta_{\sigma',\sigma}$ . Table I shows the matrix element of  $\mathcal{H}$  expressed by the basis set of  $|xy, \chi_\pm(\theta, \phi)\rangle$ ,  $|yz, \chi_\pm(\theta, \phi)\rangle$ ,  $|xz, \chi_\pm(\theta, \phi)\rangle$ ,  $|x^2 - y^2, \chi_\pm(\theta, \phi)\rangle$ , and  $|3z^2 - r^2, \chi_\pm(\theta, \phi)\rangle$ .

**Table I.** Matrix element of  $\mathcal{H}$  of Eq. (4) expressed by the basis set of  $|xy, \chi_{\pm}(\theta, \phi)\rangle$ ,  $|yz, \chi_{\pm}(\theta, \phi)\rangle$ ,  $|xz, \chi_{\pm}(\theta, \phi)\rangle$ ,  $|x^2 - y^2, \chi_{\pm}(\theta, \phi)\rangle$ , and  $|3z^2 - r^2, \chi_{\pm}(\theta, \phi)\rangle$ . The system with the crystal field of tetragonal symmetry in Fig. 2 has  $E_{xy} = 0$ ,  $E_{xz} = E_{yz} = \delta_{\zeta}$ ,  $E_{x^2 - y^2} = \Delta$ , and  $E_{3z^2 - r^2} = \Delta + \delta_{\gamma}$ . The system with the crystal field of cubic symmetry has  $E_{xy} = E_{xz} = E_{yz} = 0$  and  $E_{x^2 - y^2} = E_{3z^2 - r^2} = \Delta$ . In addition, the case of the TAMR effect has  $\phi = \pi/2$ .

	$ xy, \chi_+\rangle$	$ yz, \chi_+\rangle$	$ xz, \chi_+\rangle$	$ xy, \chi_-\rangle$	$ yz, \chi_-\rangle$	$ xz, \chi_-\rangle$	$ x^2 - y^2, \chi_+\rangle$	$ 3z^2 - r^2, \chi_+\rangle$	$ x^2 - y^2, \chi_-\rangle$	$ 3z^2 - r^2, \chi_-\rangle$
$\langle xy, \chi_+  $	$E_{xy} - \frac{H}{2}$	$i\frac{\lambda}{2} \sin \theta \sin \phi$	$-i\frac{\lambda}{2} \sin \theta \cos \phi$	0	$\frac{\lambda}{2}(e^{-i\phi} \sin^2 \frac{\theta}{2} + e^{i\phi} \cos^2 \frac{\theta}{2})$	$i\frac{\lambda}{2}(e^{-i\phi} \sin^2 \frac{\theta}{2} - e^{i\phi} \cos^2 \frac{\theta}{2})$	$i\lambda' \cos \theta$	0	$-i\lambda' \sin \theta$	0
$\langle yz, \chi_+  $	$-i\frac{\lambda}{2} \sin \theta \sin \phi$	$E_{yz} - \frac{H}{2}$	$i\frac{\lambda'}{2} \cos \theta$	$-\frac{\lambda}{2}(e^{-i\phi} \sin^2 \frac{\theta}{2} + e^{i\phi} \cos^2 \frac{\theta}{2})$	0	$-i\frac{\lambda'}{2} \sin \theta$	$-i\frac{\lambda}{2} \sin \theta \cos \phi$	$-i\frac{\sqrt{3}\lambda}{2} \sin \theta \cos \phi$	$-i\frac{\lambda}{2}(e^{-i\phi} \sin^2 \frac{\theta}{2} + e^{i\phi} \cos^2 \frac{\theta}{2})$	$-i\frac{\sqrt{3}\lambda}{2}(e^{-i\phi} \sin^2 \frac{\theta}{2} + e^{i\phi} \cos^2 \frac{\theta}{2})$
$\langle xz, \chi_+  $	$i\frac{\lambda}{2} \sin \theta \cos \phi$	$-i\frac{\lambda'}{2} \cos \theta$	$E_{xz} - \frac{H}{2}$	$-i\frac{\lambda}{2}(e^{-i\phi} \sin^2 \frac{\theta}{2} - e^{i\phi} \cos^2 \frac{\theta}{2})$	$i\frac{\lambda'}{2} \sin \theta$	0	$-i\frac{\lambda}{2} \sin \theta \sin \phi$	$i\frac{\sqrt{3}\lambda}{2} \sin \theta \sin \phi$	$-\frac{\lambda}{2}(e^{-i\phi} \sin^2 \frac{\theta}{2} + e^{i\phi} \cos^2 \frac{\theta}{2})$	$\frac{\sqrt{3}\lambda}{2}(e^{-i\phi} \sin^2 \frac{\theta}{2} + e^{i\phi} \cos^2 \frac{\theta}{2})$
$\langle xy, \chi_-  $	0	$-\frac{\lambda}{2}(e^{-i\phi} \cos^2 \frac{\theta}{2} + e^{i\phi} \sin^2 \frac{\theta}{2})$	$-i\frac{\lambda}{2}(e^{-i\phi} \cos^2 \frac{\theta}{2} - e^{i\phi} \sin^2 \frac{\theta}{2})$	$E_{xy} + \frac{H}{2}$	$-i\frac{\lambda}{2} \sin \theta \sin \phi$	$i\frac{\lambda}{2} \sin \theta \cos \phi$	$-i\lambda' \sin \theta$	0	$-i\lambda' \cos \theta$	0
$\langle yz, \chi_-  $	$\frac{\lambda}{2}(e^{-i\phi} \cos^2 \frac{\theta}{2} + e^{i\phi} \sin^2 \frac{\theta}{2})$	0	$-i\frac{\lambda'}{2} \sin \theta$	$i\frac{\lambda}{2} \sin \theta \sin \phi$	$E_{yz} + \frac{H}{2}$	$-i\frac{\lambda'}{2} \cos \theta$	$-i\frac{\lambda}{2}(e^{-i\phi} \cos^2 \frac{\theta}{2} - e^{i\phi} \sin^2 \frac{\theta}{2})$	$-i\frac{\sqrt{3}\lambda}{2}(e^{-i\phi} \cos^2 \frac{\theta}{2} - e^{i\phi} \sin^2 \frac{\theta}{2})$	$i\frac{\lambda}{2} \sin \theta \cos \phi$	$i\frac{\sqrt{3}\lambda}{2} \sin \theta \cos \phi$
$\langle xz, \chi_-  $	$i\frac{\lambda}{2}(e^{-i\phi} \cos^2 \frac{\theta}{2} - e^{i\phi} \sin^2 \frac{\theta}{2})$	$i\frac{\lambda'}{2} \sin \theta$	0	$-i\frac{\lambda}{2} \sin \theta \cos \phi$	$i\frac{\lambda'}{2} \cos \theta$	$E_{xz} + \frac{H}{2}$	$\frac{\lambda}{2}(e^{-i\phi} \cos^2 \frac{\theta}{2} + e^{i\phi} \sin^2 \frac{\theta}{2})$	$-\frac{\sqrt{3}\lambda}{2}(e^{-i\phi} \cos^2 \frac{\theta}{2} + e^{i\phi} \sin^2 \frac{\theta}{2})$	$i\frac{\lambda}{2} \sin \theta \sin \phi$	$-i\frac{\sqrt{3}\lambda}{2} \sin \theta \sin \phi$
$\langle x^2 - y^2, \chi_+  $	$-i\lambda' \cos \theta$	$i\frac{\lambda}{2} \sin \theta \cos \phi$	$i\frac{\lambda}{2} \sin \theta \sin \phi$	$i\lambda' \sin \theta$	$i\frac{\lambda}{2}(e^{-i\phi} \sin^2 \frac{\theta}{2} + e^{i\phi} \cos^2 \frac{\theta}{2})$	$\frac{\lambda}{2}(e^{-i\phi} \sin^2 \frac{\theta}{2} + e^{i\phi} \cos^2 \frac{\theta}{2})$	$E_{x^2 - y^2} - \frac{H}{2}$	0	0	0
$\langle 3z^2 - r^2, \chi_+  $	0	$i\frac{\sqrt{3}\lambda}{2} \sin \theta \cos \phi$	$-i\frac{\sqrt{3}\lambda}{2} \sin \theta \sin \phi$	0	$i\frac{\sqrt{3}\lambda}{2}(e^{-i\phi} \sin^2 \frac{\theta}{2} + e^{i\phi} \cos^2 \frac{\theta}{2})$	$-\frac{\sqrt{3}\lambda}{2}(e^{-i\phi} \sin^2 \frac{\theta}{2} + e^{i\phi} \cos^2 \frac{\theta}{2})$	0	$E_{3z^2 - r^2} - \frac{H}{2}$	0	0
$\langle x^2 - y^2, \chi_-  $	$i\lambda' \sin \theta$	$i\frac{\lambda}{2}(e^{-i\phi} \cos^2 \frac{\theta}{2} - e^{i\phi} \sin^2 \frac{\theta}{2})$	$-\frac{\lambda}{2}(e^{-i\phi} \cos^2 \frac{\theta}{2} + e^{i\phi} \sin^2 \frac{\theta}{2})$	$i\lambda' \cos \theta$	$-i\frac{\lambda}{2} \sin \theta \cos \phi$	$-i\frac{\lambda}{2} \sin \theta \sin \phi$	0	0	$E_{x^2 - y^2} + \frac{H}{2}$	0
$\langle 3z^2 - r^2, \chi_-  $	0	$i\frac{\sqrt{3}\lambda}{2}(e^{-i\phi} \cos^2 \frac{\theta}{2} - e^{i\phi} \sin^2 \frac{\theta}{2})$	$\frac{\sqrt{3}\lambda}{2}(e^{-i\phi} \cos^2 \frac{\theta}{2} + e^{i\phi} \sin^2 \frac{\theta}{2})$	0	$-i\frac{\sqrt{3}\lambda}{2} \sin \theta \cos \phi$	$i\frac{\sqrt{3}\lambda}{2} \sin \theta \sin \phi$	0	0	0	$E_{3z^2 - r^2} + \frac{H}{2}$

## 2.2 Localized d states

Applying the exact diagonalization method to  $\mathcal{H}$  of Eq. (4) (i.e., Table I), we numerically obtain the wave function of the localized d states,  $|\psi_{j,\varsigma}(\theta, \phi)\rangle$ . In this study we mainly consider the case in which  $\lambda$  is smaller than  $H$  and the crystal field energy, where the crystal field energy is  $E_{x^2-y^2} - E_{xy}$  ( $= \Delta$ ) as noted in Sect. 4.1 (see also Fig. 2). In this case,  $|\psi_{j,\varsigma}(\theta, \phi)\rangle$  is expressed as

$$|\psi_{j,\varsigma}(\theta, \phi)\rangle = \sum_{\substack{i=xy,yz,xz \\ x^2-y^2, 3z^2-r^2}} \sum_{\sigma=+,-} c_{i,\sigma}^{j,\varsigma}(\theta, \phi) |i, \chi_{\sigma}(\theta, \phi)\rangle, \quad (13)$$

with  $j = xy, yz, xz, x^2 - y^2$ , and  $3z^2 - r^2$  and  $\varsigma = +$  and  $-$ . The quantity  $c_{i,\sigma}^{j,\varsigma}(\theta, \phi)$  is the probability amplitude of  $|i, \chi_{\sigma}(\theta, \phi)\rangle$ . Here,  $j$  and  $\varsigma$  respectively specify the orbital and spin indexes of the dominant state in  $\sum_i \sum_{\sigma} c_{i,\sigma}^{j,\varsigma}(\theta, \phi) |i, \chi_{\sigma}(\theta, \phi)\rangle$ . We also mention the case in which  $\lambda$  is smaller than  $H$  but larger than the crystal field energy (e.g., the case of no crystal field in Sects. 4.1 and 4.2.1). In this case,  $j$  does not correspond well to  $xy, yz, xz, x^2 - y^2$ , and  $3z^2 - r^2$ . Therefore, we may assign a number to  $j$  in descending order of the eigenvalue of  $\mathcal{H}$ , i.e.,  $j = 1, 2, 3, 4$ , and  $5$ .

The state  $|\psi_{j,\varsigma}(\theta, \phi)\rangle$  has a normalized orthogonal system:

$$(\psi_{j',\varsigma'}(\theta, \phi) | \psi_{j,\varsigma}(\theta, \phi)) = \delta_{j',j} \delta_{\varsigma',\varsigma}, \quad (14)$$

where

$$(\psi_{j,\varsigma}(\theta, \phi) | \psi_{j,\varsigma}(\theta, \phi)) = \sum_i \sum_{\sigma} |c_{i,\sigma}^{j,\varsigma}(\theta, \phi)|^2 = 1. \quad (15)$$

Furthermore, we have the following condition:

$$\begin{aligned} & \sum_j \sum_{\varsigma} [c_{i,\sigma}^{j,\varsigma}(\theta, \phi)]^* c_{i',\sigma'}^{j,\varsigma}(\theta, \phi) \\ &= \sum_j \sum_{\varsigma} \langle i, \chi_{\sigma}(\theta, \phi) | \psi_{j,\varsigma}(\theta, \phi) \rangle^* \langle i', \chi_{\sigma'}(\theta, \phi) | \psi_{j,\varsigma}(\theta, \phi) \rangle \\ &= \sum_j \sum_{\varsigma} \langle i', \chi_{\sigma'}(\theta, \phi) | \psi_{j,\varsigma}(\theta, \phi) \rangle (\psi_{j,\varsigma}(\theta, \phi) | i, \chi_{\sigma}(\theta, \phi) \rangle) \\ &= \langle i', \chi_{\sigma'}(\theta, \phi) | i, \chi_{\sigma}(\theta, \phi) \rangle \\ &= \delta_{i',i} \delta_{\sigma',\sigma}, \end{aligned} \quad (16)$$

where the completeness,  $\sum_j \sum_{\varsigma} |\psi_{j,\varsigma}(\theta, \phi)\rangle (\psi_{j,\varsigma}(\theta, \phi) |) = 1$ , has been used. In particular,

when  $i' = i$  and  $\sigma' = \sigma$ , Eq. (16) becomes

$$\sum_j \sum_\sigma |c_{i,\sigma}^{j,\zeta}(\theta, \phi)|^2 = 1. \quad (17)$$

Equations (16) and (17) will be used in Eqs. (31) and (45).

### 2.3 Resistivity

Using  $|\psi_{j,\zeta}(\theta, \phi)\rangle$  of Eq. (13), we can obtain an expression of  $\rho(\Theta, \Phi; \theta, \phi)$ . The resistivity  $\rho(\Theta, \Phi; \theta, \phi)$  is described by the two-current model,<sup>3)</sup> i.e.,

$$\rho(\Theta, \Phi; \theta, \phi) = \frac{\rho_+(\Theta, \Phi; \theta, \phi)\rho_-(\Theta, \Phi; \theta, \phi)}{\rho_+(\Theta, \Phi; \theta, \phi) + \rho_-(\Theta, \Phi; \theta, \phi)}, \quad (18)$$

where  $\rho_\sigma(\Theta, \Phi; \theta, \phi)$  is the resistivity of the  $\sigma$  spin at  $(\Theta, \Phi)$  and  $(\theta, \phi)$ . Here,  $\sigma = +$  ( $-$ ) denotes the up spin (down spin) for the case in which the quantization axis is chosen along the direction of  $\langle \mathbf{S} \rangle$  [see Eqs. (11) and (12)]. The resistivity  $\rho_\sigma(\Theta, \Phi; \theta, \phi)$  is written as

$$\rho_\sigma(\Theta, \Phi; \theta, \phi) = \frac{m_\sigma^*}{n_\sigma e^2 \tau_\sigma(\Theta, \Phi; \theta, \phi)}, \quad (19)$$

where  $e$  is the electron charge and  $n_\sigma$  ( $m_\sigma^*$ ) is the number density (effective mass) of the electrons in the conduction band of the  $\sigma$  spin.<sup>26,27)</sup> The conduction band consists of the s, p, and conductive d states.<sup>12)</sup> In addition,  $1/\tau_\sigma(\Theta, \Phi; \theta, \phi)$  is the scattering rate of the conduction electron of the  $\sigma$  spin at  $(\Theta, \Phi)$  and  $(\theta, \phi)$ , expressed by

$$\frac{1}{\tau_\sigma(\Theta, \Phi; \theta, \phi)} = \frac{1}{\tau_{s,\sigma}} + \sum_{\substack{j=xy,yz,xz \\ x^2-y^2, 3z^2-r^2}} \sum_{\zeta=+,-} \frac{1}{\tau_{s,\sigma \rightarrow j,\zeta}(\Theta, \Phi; \theta, \phi)}, \quad (20)$$

with

$$\frac{1}{\tau_{s,\sigma \rightarrow j,\zeta}(\Theta, \Phi; \theta, \phi)} = \frac{2\pi}{\hbar} n_{\text{imp}} N_{\text{n}} V_{\text{imp}} (R_{\text{n}})^2 \left| \langle \psi_{j,\zeta}(\theta, \phi) | e^{i\mathbf{k}_\sigma \cdot \mathbf{r}}, \chi_\sigma(\theta, \phi) \rangle \right|^2 D_{j,\zeta}^{(d)}, \quad (21)$$

$$|e^{i\mathbf{k}_\sigma \cdot \mathbf{r}}, \chi_\sigma(\theta, \phi)\rangle = \frac{1}{\sqrt{\Omega}} e^{i\mathbf{k}_\sigma \cdot \mathbf{r}} \chi_\sigma(\theta, \phi), \quad (22)$$

$$\mathbf{k}_\sigma = (k_{x,\sigma}, k_{y,\sigma}, k_{z,\sigma}) = k_\sigma (\sin \Theta \cos \Phi, \sin \Theta \sin \Phi, \cos \Theta), \quad (23)$$

$$\mathbf{r} = (x, y, z), \quad (24)$$

where  $k_\sigma = |\mathbf{k}_\sigma|$ . Here,  $1/\tau_{s,\sigma}$  is the  $s$ - $s$  scattering rate, which is considered to be independent of  $(\Theta, \Phi)$  and  $(\theta, \phi)$ . The  $s$ - $s$  scattering means that the conduction electron of the  $\sigma$  spin is scattered into the conduction state of the  $\sigma$  spin by nonmagnetic impurities and phonons.<sup>15)</sup> The quantity  $1/\tau_{s,\sigma \rightarrow j,\zeta}(\Theta, \Phi; \theta, \phi)$  is the  $s$ - $d$  scattering rate



at  $(\Theta, \Phi)$  and  $(\theta, \phi)$ .<sup>12,13)</sup> The  $s$ - $d$  scattering means that the conduction electron of the  $\sigma$  spin is scattered into the  $\sigma$  spin state in  $|\psi_{j,\varsigma}(\theta, \phi)\rangle$  of Eq. (13) by nonmagnetic impurities. The conduction state of the  $\sigma$  spin  $|e^{i\mathbf{k}_\sigma \cdot \mathbf{r}}, \chi_\sigma(\theta, \phi)\rangle$  is represented by the plane wave, where  $\mathbf{k}_\sigma$  is the Fermi wave vector of the  $\sigma$  spin at  $(\Theta, \Phi)$ ,  $\mathbf{r}$  is the position of the conduction electron, and  $\Omega$  is the volume of the system. The quantity  $V_{\text{imp}}(R_n)$  is the scattering potential at  $R_n$  due to a single impurity, where  $R_n$  is the distance between the impurity and the nearest-neighbor host atom.<sup>12)</sup> The quantity  $N_n$  is the number of nearest-neighbor host atoms around a single impurity,<sup>12)</sup>  $n_{\text{imp}}$  is the number density of impurities, and  $\hbar$  is the Planck constant  $h$  divided by  $2\pi$ . The quantity  $D_{j,\varsigma}^{(d)}$  represents the partial density of states (PDOS) of the wave function of the tight-binding model for the  $d$  state of the  $j$  orbital and  $\varsigma$  spin at  $E_F$ , as described in Appendix B in Ref. 12.

Substituting  $|\psi_{j,\varsigma}(\theta, \phi)\rangle$  of Eq. (13) into  $1/\tau_{s,\sigma \rightarrow j,\varsigma}(\Theta, \Phi; \theta, \phi)$  of Eq. (21) we can rewrite  $\sum_j \sum_\varsigma 1/\tau_{s,\sigma \rightarrow j,\varsigma}(\Theta, \Phi; \theta, \phi)$  in Eq. (20) as<sup>28)</sup>

$$\sum_j \sum_\varsigma \frac{1}{\tau_{s,\sigma \rightarrow j,\varsigma}(\Theta, \Phi; \theta, \phi)} = \frac{2\pi}{\hbar} n_{\text{imp}} N_n v_\sigma^2 \sum_j \sum_\varsigma P_\sigma^{j,\varsigma}(\Theta, \Phi; \theta, \phi) D_{j,\varsigma}^{(d)}, \quad (25)$$

with

$$v_\sigma = V_{\text{imp}}(R_n) g_\sigma, \quad (26)$$

$$g_\sigma = -\frac{192\pi\Gamma\zeta k_\sigma^2}{\sqrt{\Omega}(k_\sigma^2 + \zeta^2)^4}, \quad (27)$$

$$P_\sigma^{j,\varsigma}(\Theta, \Phi; \theta, \phi) = |\varphi_\sigma^{j,\varsigma}(\Theta, \Phi; \theta, \phi)|^2, \quad (28)$$

$$\begin{aligned} \varphi_\sigma^{j,\varsigma}(\Theta, \Phi; \theta, \phi) = & c_{xy,\sigma}^{j,\varsigma}(\theta, \phi) x_0 y_0 + c_{yz,\sigma}^{j,\varsigma}(\theta, \phi) y_0 z_0 + c_{xz,\sigma}^{j,\varsigma}(\theta, \phi) x_0 z_0 \\ & + c_{x^2-y^2,\sigma}^{j,\varsigma}(\theta, \phi) \frac{1}{2}(x_0^2 - y_0^2) + c_{3z^2-r^2,\sigma}^{j,\varsigma}(\theta, \phi) \frac{1}{2\sqrt{3}}(3z_0^2 - r_0^2), \end{aligned} \quad (29)$$

where  $x_0 = \sin \Theta \cos \Phi$ ,  $y_0 = \sin \Theta \sin \Phi$ ,  $z_0 = \cos \Theta$ , and  $r_0 = 1$ . Here,  $c_{i,\sigma}^{j,\varsigma}(\theta, \phi)$  is numerically obtained by applying the exact diagonalization method to  $\mathcal{H}$  of Eq. (4) [also see Eq. (13)]. The quantity  $\varphi_\sigma^{j,\varsigma}(\Theta, \Phi; \theta, \phi)$  is proportional to the probability amplitude of the  $d$  states of the  $\sigma$  spin of the  $\mathbf{I}$  direction (i.e., the  $\mathbf{k}_\sigma/k_\sigma$  direction) in  $|\psi_{j,\varsigma}(\theta, \phi)\rangle$  of Eq. (13). In addition,  $P_\sigma^{j,\varsigma}(\Theta, \Phi; \theta, \phi)$  is proportional to the probability density of the  $d$  states of the  $\sigma$  spin of the  $\mathbf{I}$  direction in  $|\psi_{j,\varsigma}(\theta, \phi)\rangle$  of Eq. (13). We emphasize that  $|\langle \psi_{j,\varsigma}(\theta, \phi) | e^{i\mathbf{k}_\sigma \cdot \mathbf{r}}, \chi_\sigma(\theta, \phi) \rangle|^2$  in Eq. (21) is finally expressed by  $P_\sigma^{j,\varsigma}(\Theta, \Phi; \theta, \phi)$ .

Using Eqs. (1), (18)–(20), and (25)–(29), we can calculate  $\text{AMR}(\Theta, \Phi; \theta, \phi)$  of Eq. (1) for various ferromagnets. As a check, we now examine  $\text{AMR}(\Theta, \Phi; \theta, \phi)$  for a system with a constant PDOS, i.e.,  $D_{j,\varsigma}^{(d)} \equiv D^{(d)}$ , where  $D^{(d)}$  is the constant. In this system,

$\sum_j \sum_\varsigma 1/\tau_{s,\sigma \rightarrow j,\varsigma}(\Theta, \Phi; \theta, \phi)$  of Eq. (25) becomes constant, i.e.,

$$\sum_j \sum_\varsigma \frac{1}{\tau_{s,\sigma \rightarrow j,\varsigma}(\Theta, \Phi; \theta, \phi)} = \frac{2\pi}{\hbar} n_{\text{imp}} N_n v_\sigma^2 \frac{D^{(d)}}{3}. \quad (30)$$

Here, Eq. (30) is obtained by using the following condition:

$$\sum_j \sum_\varsigma P_\sigma^{j,\varsigma}(\Theta, \Phi; \theta, \phi) = \frac{1}{3}, \quad (31)$$

which is derived from Eqs. (28), (29), and the condition of Eq. (16). As a result, the system exhibits  $\text{AMR}(\Theta, \Phi; \theta, \phi) = 0$ .

### 3. Application to TAMR effect

We apply the theory presented in Sect. 2 to the TAMR effect of  $\mathbf{I}//[100]$  and  $\mathbf{M}$  in the (100) plane for ferromagnets. This case has  $\Theta = \pi/2$ ,  $\Phi = 0$ , and  $\phi = \pi/2$ . Here, we introduce the following quantities for Eqs. (11)–(13), (19), (21), and (28):

$$\chi_\sigma(\theta, \pi/2) \equiv \chi_\sigma(\theta), \quad (32)$$

$$|\psi_{j,\varsigma}(\theta, \pi/2)\rangle \equiv |\psi_{j,\varsigma}(\theta)\rangle, \quad (33)$$

$$c_{i,\sigma}^{j,\varsigma}(\theta, \pi/2) \equiv c_{i,\sigma}^{j,\varsigma}(\theta), \quad (34)$$

$$\rho_\sigma(\pi/2, 0; \theta, \pi/2) \equiv \rho_\sigma(\theta), \quad (35)$$

$$\frac{1}{\tau_{s,\sigma \rightarrow j,\varsigma}(\pi/2, 0; \theta, \pi/2)} \equiv \frac{1}{\tau_{s,\sigma \rightarrow j,\varsigma}(\theta)}, \quad (36)$$

$$P_\sigma^{j,\varsigma}(\pi/2, 0; \theta, \pi/2) \equiv P_\sigma^{j,\varsigma}(\theta). \quad (37)$$

#### 3.1 Coefficients

When  $\text{TAMR}(\theta)$  of Eq. (2) is expressed as Eq. (3), we determine  $C_0$  to be  $-C_2 - C_4$  from the following relation:

$$\text{TAMR}(0) = C_0 + C_2 + C_4 = 0. \quad (38)$$

In addition,  $C_2$  and  $C_4$  are obtained from the following equations:

$$\text{TAMR}(\pi/4) = -C_2 - 2C_4 = f_{\pi/4}, \quad (39)$$

$$\text{TAMR}(\pi/2) = -2C_2 = f_{\pi/2}, \quad (40)$$

where  $f_{\pi/4}$  and  $f_{\pi/2}$ , respectively, represent the numerical values of  $\text{TAMR}(\pi/4)$  and  $\text{TAMR}(\pi/2)$  calculated by applying the theory presented in Sect. 2. The coefficients  $C_2$

and  $C_4$  are therefore expressed as

$$C_2 = -\frac{1}{2}f_{\pi/2}, \quad (41)$$

$$C_4 = \frac{1}{4}f_{\pi/2} - \frac{1}{2}f_{\pi/4}. \quad (42)$$

### 3.2 Probability density

Substituting  $\Theta = \pi/2$ ,  $\Phi = 0$ , and  $\phi = \pi/2$  into Eqs. (28) and (29), we obtain  $P_\sigma^{j,\varsigma}(\theta)$  of Eq. (37) as

$$P_\sigma^{j,\varsigma}(\theta) = |\varphi_\sigma^{j,\varsigma}(\pi/2, 0; \theta, \pi/2)|^2, \quad (43)$$

with

$$\varphi_\sigma^{j,\varsigma}(\pi/2, 0; \theta, \pi/2) = \frac{1}{2}c_{x^2-y^2,\sigma}^{j,\varsigma}(\theta) - \frac{1}{2\sqrt{3}}c_{3z^2-r^2,\sigma}^{j,\varsigma}(\theta), \quad (44)$$

where Eq. (34) has been used. Here,  $\varphi_\sigma^{j,\varsigma}(\pi/2, 0; \theta, \pi/2)$  is proportional to the probability amplitude of the  $d\gamma$  states of the  $\sigma$  spin of the  $\mathbf{I}$  direction ( $x$  direction) in  $|\psi_{j,\varsigma}(\theta)\rangle$  of Eqs. (13) and (33), where the  $d\gamma$  states of the  $\sigma$  spin consist of  $|x^2 - y^2, \chi_\sigma(\theta)\rangle$  and  $|3z^2 - r^2, \chi_\sigma(\theta)\rangle$ . The  $d\gamma$  states of the  $\sigma$  spin of the  $\mathbf{I}$  direction ( $x$  direction) are called “ $d\gamma_{x,\sigma}$  states” hereafter. The quantity  $P_\sigma^{j,\varsigma}(\theta)$  of Eq. (43) is proportional to the probability density of the  $d\gamma_{x,\sigma}$  states in  $|\psi_{j,\varsigma}(\theta)\rangle$  of Eqs. (13) and (33).

As shown in Eq. (31),  $P_\sigma^{j,\varsigma}(\theta)$  of Eq. (43) also has the following condition:

$$\sum_j \sum_\varsigma P_\sigma^{j,\varsigma}(\theta) = \frac{1}{3}. \quad (45)$$

Equation (45) will be used in Sects. 4.2.2 and 4.2.3.

## 4. TAMR effect for strong ferromagnets

We numerically calculate  $C_2$  of Eq. (41),  $C_4$  of Eq. (42), and TAMR( $\theta$ ) of Eq. (2) for strong ferromagnets with  $D_{j,+}^{(d)} = 0$  and  $\sum_j D_{j,-}^{(d)} \neq 0$ .<sup>23)</sup> We here consider three cases of crystal field: no crystal field, the crystal field of cubic symmetry, and the crystal field of tetragonal symmetry.<sup>29)</sup> In the case of tetragonal symmetry, a tetragonal distortion exists in the [001] direction.

### 4.1 Systems and parameters

We describe the system and parameters for the calculation.

In Fig. 2, we show the energy levels of the d states in the crystal field of tetragonal symmetry.<sup>29)</sup> The states  $|xy, \chi_\sigma(\theta)\rangle$ ,  $|yz, \chi_\sigma(\theta)\rangle$ , and  $|xz, \chi_\sigma(\theta)\rangle$  are called  $d\varepsilon$  states and  $|x^2 - y^2, \chi_\sigma(\theta)\rangle$  and  $|3z^2 - r^2, \chi_\sigma(\theta)\rangle$  are  $d\gamma$  states. The quantity  $\Delta$  is the energy level of

$|x^2 - y^2, \chi_\sigma(\theta)\rangle$  measured from that of  $|xy, \chi_\sigma(\theta)\rangle$ , i.e.,  $\Delta = E_{x^2-y^2} - E_{xy}$ . The quantity  $\delta_\varepsilon$  is the energy level of  $|xz, \chi_\sigma(\theta)\rangle$  (or  $|yz, \chi_\sigma(\theta)\rangle$ ) measured from that of  $|xy, \chi_\sigma(\theta)\rangle$ , i.e.,  $\delta_\varepsilon = E_{xz} - E_{xy} = E_{yz} - E_{xy}$ . The quantity  $\delta_\gamma$  is the energy level of  $|3z^2 - r^2, \chi_\sigma(\theta)\rangle$  measured from that of  $|x^2 - y^2, \chi_\sigma(\theta)\rangle$ , i.e.,  $\delta_\gamma = E_{3z^2-r^2} - E_{x^2-y^2}$ . Also note that the crystal field of cubic symmetry corresponds to the case of  $\delta_\varepsilon = \delta_\gamma = 0$ .<sup>29)</sup>

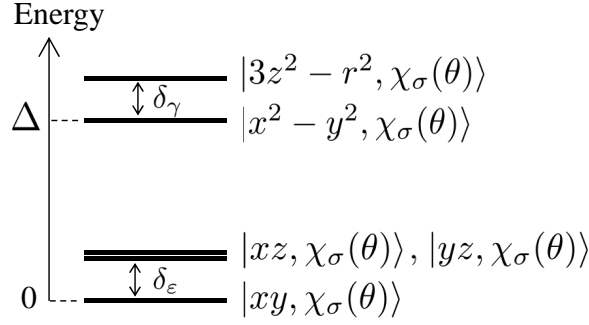


**Fig. 2.** Energy levels of the d states in the crystal field of tetragonal symmetry.<sup>29)</sup> The second excited states are doubly degenerate. The energy levels are measured from the energy level of  $|xy, \chi_\sigma(\theta)\rangle$ . The energy levels of the d states in the crystal field of cubic symmetry correspond to the case of  $\delta_\varepsilon = \delta_\gamma = 0$ .<sup>29)</sup>

In accordance with our previous study,<sup>13)</sup> we introduce the following quantities:

$$r = \frac{\rho_{s,-}}{\rho_{s,+}}, \quad (46)$$

$$r_{s,\sigma \rightarrow j,\varsigma} = \frac{\rho_{s,\sigma \rightarrow j,\varsigma}}{\rho_{s,+}}, \quad (47)$$

with

$$\rho_{s,\sigma} = \frac{m_\sigma^*}{n_\sigma e^2 \tau_{s,\sigma}}, \quad (48)$$

$$\rho_{s,\sigma \rightarrow j,\varsigma} = \frac{m_\sigma^*}{n_\sigma e^2 \tau_{s,\sigma \rightarrow j,\varsigma}^{(0)}}, \quad (49)$$

where  $\rho_{s,\sigma}$  is the  $s$ - $s$  resistivity and  $\rho_{s,\sigma \rightarrow j,\varsigma}$  is the  $s$ - $d$  resistivity. Here,  $1/\tau_{s,\sigma \rightarrow j,\varsigma}^{(0)}$  is the  $s$ - $d$  scattering rate<sup>30)</sup> given by

$$\frac{1}{\tau_{s,\sigma \rightarrow j,\varsigma}^{(0)}} = \frac{2\pi}{\hbar} n_{\text{imp}} N_n \frac{1}{3} v_\sigma^2 D_{j,\varsigma}^{(d)}. \quad (50)$$

As a result,  $r_{s,\sigma \rightarrow j,\varsigma}$  of Eq. (47) has

$$r_{s,\sigma \rightarrow j,\varsigma} \propto D_{j,\varsigma}^{(d)}. \quad (51)$$

In addition to the above-mentioned  $D_{j,+}^{(d)} = 0$ ,  $D_{j,-}^{(d)}$  is set to be

$$D_{xy,-}^{(d)} \equiv D_{\varepsilon 1,-}^{(d)}, \quad (52)$$

$$D_{xz,-}^{(d)} = D_{yz,-}^{(d)} \equiv D_{\varepsilon 2,-}^{(d)}, \quad (53)$$

$$D_{x^2-y^2,-}^{(d)} \equiv D_{\gamma 1,-}^{(d)}, \quad (54)$$

$$D_{3z^2-r^2,-}^{(d)} \equiv D_{\gamma 2,-}^{(d)}, \quad (55)$$

on the basis of the energy levels in Fig. 2. Using Eqs. (47)–(55), we then have

$$r_{s,\sigma \rightarrow xy,-} \equiv r_{s,\sigma \rightarrow \varepsilon 1,-}, \quad (56)$$

$$r_{s,\sigma \rightarrow xz,-} = r_{s,\sigma \rightarrow yz,-} \equiv r_{s,\sigma \rightarrow \varepsilon 2,-}, \quad (57)$$

$$r_{s,\sigma \rightarrow x^2-y^2,-} \equiv r_{s,\sigma \rightarrow \gamma 1,-}, \quad (58)$$

$$r_{s,\sigma \rightarrow 3z^2-r^2,-} \equiv r_{s,\sigma \rightarrow \gamma 2,-}, \quad (59)$$

and also  $r_{s,\sigma \rightarrow j,+} = 0$ . Actually, there may be a difference in the values between  $D_{\varepsilon 1,-}^{(d)}$  and  $D_{\varepsilon 2,-}^{(d)}$  or between  $D_{\gamma 1,-}^{(d)}$  and  $D_{\gamma 2,-}^{(d)}$ , as found from the energy levels in Fig. 2. In this study, however, we ignore such a difference under the assumption of  $|D_{\varepsilon 1,-}^{(d)} - D_{\varepsilon 2,-}^{(d)}|/D_{\varepsilon 1,-}^{(d)} \ll 1$  and  $|D_{\gamma 1,-}^{(d)} - D_{\gamma 2,-}^{(d)}|/D_{\gamma 1,-}^{(d)} \ll 1$ , which may be valid for the parameters with  $\delta \sim \lambda < \Delta \ll H$  mentioned later. Namely, we set

$$D_{\varepsilon 1,-}^{(d)} = D_{\varepsilon 2,-}^{(d)} \equiv D_{\varepsilon,-}^{(d)}, \quad (60)$$

$$D_{\gamma 1,-}^{(d)} = D_{\gamma 2,-}^{(d)} \equiv D_{\gamma,-}^{(d)}, \quad (61)$$

and

$$r_{s,\sigma \rightarrow \varepsilon 1,-} = r_{s,\sigma \rightarrow \varepsilon 2,-} \equiv r_{s,\sigma \rightarrow \varepsilon,-}, \quad (62)$$

$$r_{s,\sigma \rightarrow \gamma 1,-} = r_{s,\sigma \rightarrow \gamma 2,-} \equiv r_{s,\sigma \rightarrow \gamma,-}. \quad (63)$$

In addition, in a conventional manner,<sup>31)</sup> we consider a simple system with  $n_+ = n_-$ ,  $m_+^* = m_-^*$ , and  $v_+ = v_-$ , where  $v_+ = v_-$  is satisfied by setting  $k_+ = k_-$  in Eqs. (26) and (27). In this system,  $r_{s,\sigma \rightarrow j,-}$  of Eq. (47) is independent of  $\sigma$ . We also introduce the following quantities:

$$P_{\sigma}^{d\varepsilon,-}(\theta) = P_{\sigma}^{xy,-}(\theta) + P_{\sigma}^{yz,-}(\theta) + P_{\sigma}^{xz,-}(\theta), \quad (64)$$

$$P_{\sigma}^{d\gamma,-}(\theta) = P_{\sigma}^{x^2-y^2,-}(\theta) + P_{\sigma}^{3z^2-r^2,-}(\theta), \quad (65)$$

where  $P_{\sigma}^{j,\varsigma}(\theta)$  has been given by Eq. (43). The quantity  $P_{\sigma}^{d\varepsilon,-}(\theta)$  is proportional to the sum of the probability densities of the  $d\gamma_{x,\sigma}$  states in  $|\psi_{xy,-}(\theta)\rangle$ ,  $|\psi_{yz,-}(\theta)\rangle$ , and

$|\psi_{xz,-}(\theta)\rangle$ . The quantity  $P_{\sigma}^{d\gamma,-}(\theta)$  is proportional to the sum of the probability densities of the  $d\gamma_{x,\sigma}$  states in  $|\psi_{x^2-y^2,-}(\theta)\rangle$  and  $|\psi_{3z^2-r^2,-}(\theta)\rangle$ .

As common parameters, we set  $H = 1$  eV,  $\lambda = \lambda' = 0.05$  eV, and  $r = 0.001$  bearing a typical strong ferromagnet in mind.<sup>32)</sup> In addition, the system with no crystal field has  $\Delta = \delta_{\varepsilon} = \delta_{\gamma} = 0$  and the identical  $D_{j,-}^{(d)}$  for  $j = 1, 2, 3, 4,$  and  $5$ . On the basis of the identical  $D_{j,-}^{(d)}$  and our previous study,<sup>32)</sup>  $r_{s,\sigma \rightarrow j,-}$  of Eqs. (47) and (51) is set to be  $0.01$  for  $j = 1, 2, 3, 4,$  and  $5$ . The system with the crystal field of cubic symmetry has  $\Delta = 0.1$  eV and  $\delta_{\varepsilon} = \delta_{\gamma} = 0$ .<sup>32)</sup> For the system with the crystal field of tetragonal symmetry, we have  $\Delta = 0.1$  eV and, for simplicity, set

$$\delta_{\varepsilon} = \delta_{\gamma} \equiv \delta. \quad (66)$$

The value of  $\delta$  is assumed to be the same as that of  $\lambda$ , i.e.,  $0.05$  eV. We also consider three models for the cubic or tetragonal system: the  $d\varepsilon$ ,  $d\gamma$ , and  $d\varepsilon + d\gamma$  models. The  $d\varepsilon$  model has  $r_{s,\sigma \rightarrow \varepsilon,-} = 0.01$  (Ref. 32) and  $r_{s,\sigma \rightarrow \gamma,-} = 0$ , which indicate  $D_{\varepsilon,-}^{(d)} \neq 0$  and  $D_{\gamma,-}^{(d)} = 0$ , respectively. The  $d\gamma$  model has  $r_{s,\sigma \rightarrow \varepsilon,-} = 0$  and  $r_{s,\sigma \rightarrow \gamma,-} = 0.01$ , which indicate  $D_{\varepsilon,-}^{(d)} = 0$  and  $D_{\gamma,-}^{(d)} \neq 0$ , respectively. The  $d\varepsilon + d\gamma$  model has the following three types. The first type is  $r_{s,\sigma \rightarrow \gamma,-} = 0.01$  and  $r_{s,\sigma \rightarrow \varepsilon,-} = 0.005$ , i.e.,  $D_{\varepsilon,-}^{(d)}/D_{\gamma,-}^{(d)} = 0.5$ . The second type is  $r_{s,\sigma \rightarrow \gamma,-} = r_{s,\sigma \rightarrow \varepsilon,-} = 0.01$ , i.e.,  $D_{\varepsilon,-}^{(d)}/D_{\gamma,-}^{(d)} = 1$ . The third type is  $r_{s,\sigma \rightarrow \gamma,-} = 0.01$  and  $r_{s,\sigma \rightarrow \varepsilon,-} = 0.015$ , i.e.,  $D_{\varepsilon,-}^{(d)}/D_{\gamma,-}^{(d)} = 1.5$ .

## 4.2 Calculation result and consideration

We find that the cubic system exhibits the fourfold symmetric TAMR effect, while the tetragonal system shows the twofold and fourfold symmetric TAMR effect.

### 4.2.1 No crystal field

The system with no crystal field of  $\Delta = \delta = 0$  exhibits  $C_2 = C_4 = 0$  and  $\text{TAMR}(\theta) = 0$ . This result agrees with that of our previous study based on the perturbation theory.<sup>33)</sup>

### 4.2.2 Crystal field of cubic symmetry

We consider the system with the crystal field of cubic symmetry. In Fig. 3, we show the  $D_{\varepsilon,-}^{(d)}/D_{\gamma,-}^{(d)}$  ( $= r_{s,\sigma \rightarrow \varepsilon,-}/r_{s,\sigma \rightarrow \gamma,-}$ ) dependence of  $C_2$  of Eq. (41) [ $C_4$  of Eq. (42)] for the system with  $r_{s,+ \rightarrow \gamma,-} = r_{s,- \rightarrow \gamma,-} = 0.01$  by the solid black line [dashed black curve]. We find that the system has  $C_2 = 0$  regardless of  $D_{\varepsilon,-}^{(d)}/D_{\gamma,-}^{(d)}$ . In addition, the system shows  $C_4 > 0$  for  $D_{\varepsilon,-}^{(d)}/D_{\gamma,-}^{(d)} < 1$ ,  $C_4 = 0$  at  $D_{\varepsilon,-}^{(d)}/D_{\gamma,-}^{(d)} = 1$ , and  $C_4 < 0$  for  $D_{\varepsilon,-}^{(d)}/D_{\gamma,-}^{(d)} > 1$ .

By using  $C_2 = 0$  and Eq. (38),  $\text{TAMR}(\theta)$  of Eq. (3) is rewritten as

$$\text{TAMR}(\theta) = C_4(-1 + \cos 4\theta). \quad (67)$$

The system therefore exhibits the fourfold symmetric TAMR effect with  $\text{TAMR}(\theta) \leq 0$  for  $D_{\varepsilon,-}^{(d)}/D_{\gamma,-}^{(d)} < 1$  and  $\text{TAMR}(\theta) \geq 0$  for  $D_{\varepsilon,-}^{(d)}/D_{\gamma,-}^{(d)} > 1$ , while the system has  $\text{TAMR}(\theta) = 0$  at  $D_{\varepsilon,-}^{(d)}/D_{\gamma,-}^{(d)} = 1$ .

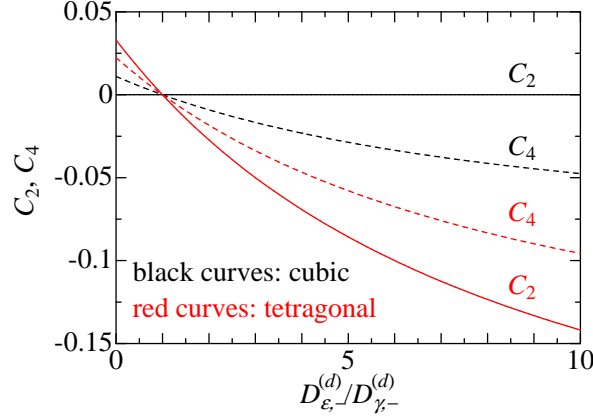


**Fig. 3.** (Color online) The quantity  $D_{\varepsilon,-}^{(d)}/D_{\gamma,-}^{(d)}$  ( $= r_{s,\sigma \rightarrow \varepsilon,-}/r_{s,\sigma \rightarrow \gamma,-}$ ) dependences of  $C_2$  and  $C_4$  for a strong ferromagnet with a crystal field of cubic symmetry or tetragonal symmetry. The system has  $D_{j,+}^{(d)} = 0$  (i.e.,  $r_{s,\sigma \rightarrow j,+} = 0$ ),  $r_{s,\sigma \rightarrow \gamma,-} = 0.01$ ,  $r = 0.001$ ,  $H = 1$  eV,  $\lambda = \lambda' = 0.05$  eV, and  $\Delta = 0.1$  eV. In addition, the system with a crystal field of cubic (tetragonal) symmetry has  $\delta = 0$  eV ( $\delta = 0.05$  eV). The result for the cubic (tetragonal) system is indicated by the black (red) curves. The coefficient  $C_2$  is represented by the solid line or curve, and  $C_4$  is shown by the dashed curve.

In Fig. 4(a), we show the  $\theta$  dependence of  $\text{TAMR}(\theta)$  of Eq. (2) for the  $d\varepsilon$ ,  $d\gamma$ , and  $d\varepsilon + d\gamma$  models. The curves represent results calculated directly by the exact diagonalization method. The dots show results obtained by substituting the evaluated  $C_4$ s of Eq. (42) into  $\text{TAMR}(\theta)$  of Eq. (67), where  $C_4$  for each model is given in Table II. We find contradictory behavior of  $\text{TAMR}(\theta)$  between the  $d\varepsilon$  model and  $d\gamma$  model. Namely, the  $d\varepsilon$  model exhibits  $\text{TAMR}(\theta) \geq 0$  with the highest value 0.11 at  $\theta = \frac{\pi}{4} + \frac{n\pi}{2}$  and the lowest value 0 at  $\theta = \frac{n\pi}{2}$ , where  $n = 0, \pm 1, \pm 2, \dots$ . In contrast, the  $d\gamma$  model shows  $\text{TAMR}(\theta) \leq 0$  with the highest value 0 at  $\theta = \frac{n\pi}{2}$  and the lowest value  $-0.022$  at  $\theta = \frac{\pi}{4} + \frac{n\pi}{2}$ , where  $n = 0, \pm 1, \pm 2, \dots$ . The  $d\varepsilon + d\gamma$  model takes  $\text{TAMR}(\theta)$  between  $\text{TAMR}(\theta)$  of the  $d\varepsilon$  model and that of the  $d\gamma$  model. Namely, the  $d\varepsilon + d\gamma$  model has  $0 \leq \text{TAMR}(\theta) \leq 0.0095$  for  $D_{\varepsilon,-}^{(d)}/D_{\gamma,-}^{(d)} = 1.5$ ,  $\text{TAMR}(\theta) = 0$  at  $D_{\varepsilon,-}^{(d)}/D_{\gamma,-}^{(d)} = 1$ , and  $-0.011 \leq \text{TAMR}(\theta) \leq 0$  for  $D_{\varepsilon,-}^{(d)}/D_{\gamma,-}^{(d)} = 0.5$ . Roughly speaking, the positive and large

TAMR( $\theta$ ) for the  $d\varepsilon$  model is reduced with the addition of the negative TAMR( $\theta$ ) for the  $d\gamma$  model [see Eq. (B·5)].

**Table II.** The coefficient  $C_4$  of Eq. (42) for strong ferromagnets with a crystal field of cubic symmetry. The system has  $D_{j,+}^{(d)} = 0$  (i.e.,  $r_{s,\sigma \rightarrow j,+} = 0$ ),  $r = 0.001$ ,  $H = 1$  eV,  $\lambda = \lambda' = 0.05$  eV, and  $\Delta = 0.1$  eV. For these systems, we consider  $d\varepsilon$ ,  $d\gamma$ , and  $d\varepsilon + d\gamma$  models. In particular, the  $d\varepsilon + d\gamma$  model has  $D_{\varepsilon,-}^{(d)}/D_{\gamma,-}^{(d)} = 0.5, 1,$  and  $1.5$ . Note that  $C_2$  of Eq. (41) is evaluated to be 0. Also, TAMR( $\theta$ ) of Eq. (67) with each  $C_4$  in this table is indicated by the dots in Fig. 4(a).

Model	$C_4$
$d\varepsilon$	-0.054
$d\gamma$	0.011
$d\varepsilon + d\gamma$ ( $D_{\varepsilon,-}^{(d)}/D_{\gamma,-}^{(d)} = 0.5$ )	0.0053
$d\varepsilon + d\gamma$ ( $D_{\varepsilon,-}^{(d)}/D_{\gamma,-}^{(d)} = 1$ )	0
$d\varepsilon + d\gamma$ ( $D_{\varepsilon,-}^{(d)}/D_{\gamma,-}^{(d)} = 1.5$ )	-0.0048

The  $\theta$  dependences of TAMR( $\theta$ ) for the  $d\varepsilon$  and  $d\gamma$  models directly reflect those of  $P_-^{d\varepsilon,-}(\theta)$  and  $P_-^{d\gamma,-}(\theta)$ , respectively, as found from Eqs. (A·1)–(A·3), (B·1), and (B·2). In particular, the contradictory behavior of TAMR( $\theta$ ) between the  $d\varepsilon$  model and the  $d\gamma$  model arises under the condition of  $P_-^{d\varepsilon,-}(\theta) + P_-^{d\gamma,-}(\theta) \approx 1/3$  of Eq. (C·2). In Fig. 4(b) [(c)], we first show the  $\theta$  dependences of  $P_-^{d\varepsilon,-}(\theta)$  [ $P_-^{d\gamma,-}(\theta)$ ] by the black curve. We find contradictory behavior between  $P_-^{d\varepsilon,-}(\theta)$  and  $P_-^{d\gamma,-}(\theta)$ , in which  $P_-^{d\gamma,-}(\theta)$  decreases (increases) as  $P_-^{d\varepsilon,-}(\theta)$  increases (decreases). Next, the  $\theta$  dependences of  $P_-^{d\varepsilon,-}(\theta) + P_-^{d\gamma,-}(\theta)$  are shown in Fig. 4(d). We confirm that  $P_-^{d\varepsilon,-}(\theta) + P_-^{d\gamma,-}(\theta)$  takes the constant value,  $1/3$ ; that is, the condition of Eq. (C·2) is satisfied.

The value of TAMR( $\theta$ ) for the  $d\varepsilon + d\gamma$  model is checked on the basis of the approximate expression of TAMR( $\theta$ ) of Eqs. (B·1)–(B·5). As shown in Eq. (B·8), TAMR( $\theta$ ) of Eq. (B·5) is less than or equal to that for the  $d\varepsilon$  model of Eq. (B·1) and greater than or equal to that for the  $d\gamma$  model of Eq. (B·2). In particular, when  $D_{\varepsilon,-}^{(d)}/D_{\gamma,-}^{(d)} = 1$ , TAMR( $\theta$ ) of Eq. (B·3) or (B·4) becomes 0 [see Eq. (B·9)].

We describe the details of  $P_-^{d\varepsilon,-}(\theta)$  of Eq. (64) for the  $d\varepsilon$  model [see Fig. 4(b)]. The quantity  $P_-^{d\varepsilon,-}(\theta)$  has peaks at  $\theta = \pi/4 + n\pi/2$ , with  $n = \pm 0, \pm 1, \pm 2, \dots$ . The peaks come from  $P_-^{xy,-}(\pi/4 + n\pi/2)$ ,  $P_-^{yz,-}(\pi/4 + n\pi/2)$ , and  $P_-^{xz,-}(\pi/4 + n\pi/2)$ . Namely, the  $d\varepsilon$  states consisting of  $|xy, \chi_-(\theta)\rangle$ ,  $|yz, \chi_-(\theta)\rangle$ , and  $|xz, \chi_-(\theta)\rangle$  are strongly hybridized to the  $d\gamma_{x,-}$  states at  $\theta = \pi/4 + n\pi/2$ . On the other hand,  $P_-^{d\varepsilon,-}(n\pi)$  [ $P_-^{d\varepsilon,-}(\pi/2 + n\pi)$ ]



is formed by only  $P_-^{xy,-}(n\pi)$  [ $P_-^{xz,-}(\pi/2 + n\pi)$ ], where  $n = 0, \pm 1, \pm 2, \dots$ . In short, only  $|xy, \chi_-(\theta)\rangle$  [ $|xz, \chi_-(\theta)\rangle$ ] in the  $d\varepsilon$  states is hybridized to the  $d\gamma_{x,-}$  states at  $\theta = n\pi$  [ $\pi/2 + n\pi$ ]. In fact, when the magnetic quantum number is represented by  $m$ ,  $|xy, \chi_-(n\pi)\rangle$  with  $m = -2$  and  $2$  (Ref. 34) is coupled to  $|x^2 - y^2, \chi_-(n\pi)\rangle$  with  $m = -2$  and  $2$  through the  $\lambda' L_z S_z$  term, as found from  $\langle x^2 - y^2, \chi_-(n\pi) | \mathcal{H} | xy, \chi_-(n\pi) \rangle = i\lambda'(-1)^n$  (see  $\mathcal{H}$  of Table I). In addition,  $|xz, \chi_-(\pi/2 + n\pi)\rangle$  with  $m = -1$  and  $1$  is coupled to  $|x^2 - y^2, \chi_-(\pi/2 + n\pi)\rangle$  with  $m = -2$  and  $2$  and  $|3z^2 - r^2, \chi_-(\pi/2 + n\pi)\rangle$  with  $m = 0$  through the  $\lambda(L_x S_x + L_y S_y)$  term (the so-called mixing term), as seen from  $\langle x^2 - y^2, \chi_-(\pi/2 + n\pi) | \mathcal{H} | xz, \chi_-(\pi/2 + n\pi) \rangle = -i(\lambda/2)(-1)^n$  and  $\langle 3z^2 - r^2, \chi_-(\pi/2 + n\pi) | \mathcal{H} | xz, \chi_-(\pi/2 + n\pi) \rangle = i(\sqrt{3}\lambda/2)(-1)^n$ . As for the respective maximum values of  $P_-^{j,-}(\theta)$ , we find  $P_-^{xz,-}(\pi/2 + n\pi) = P_-^{xy,-}(n\pi) > P_-^{yz,-}(\pi/4 + n\pi/2)$ . This relation is attributed to the probability density of the  $d\gamma_{x,-}$  states for the cubic system [see Eqs. (43) and (44)]. Namely, in the case of the cubic system, the probability density of the  $d\gamma_{x,-}$  states in  $|xz, \chi_-(\pi/2 + n\pi)\rangle$  is the same as that in  $|xy, \chi_-(n\pi)\rangle$ , whereas the probability density of the  $d\gamma_{x,-}$  states in  $|yz, \chi_-(\pi/4 + n\pi/2)\rangle$  is smaller than that in  $|xy, \chi_-(n\pi)\rangle$ .

We give the details of  $P_-^{d\gamma,-}(\theta)$  of Eq. (65) for the  $d\gamma$  model [see Fig. 4(c)]. The quantity  $P_-^{d\gamma,-}(\theta)$  has peaks at  $\theta = n\pi/2$ , with  $n = 0, \pm 1, \pm 2, \dots$ . The peaks come from  $P_-^{x^2-y^2,-}(n\pi/2)$  and  $P_-^{3z^2-r^2,-}(n\pi/2)$ . Namely, the  $d\gamma$  states consisting of  $|\psi_{x^2-y^2,-}(\theta)\rangle$  and  $|\psi_{3z^2-r^2,-}(\theta)\rangle$  include the  $d\gamma_{x,-}$  states with the highest probability density at  $\theta = n\pi/2$ . In addition, we find the characteristic relation of  $P_-^{3z^2-r^2,-}(\pi/2 + n\pi) = P_-^{x^2-y^2,-}(n\pi)$ , even though the coefficient “ $1/(2\sqrt{3})$ ” of  $c_{3z^2-r^2,-}^{3z^2-r^2,-}(\pi/2 + n\pi)$  in  $P_-^{3z^2-r^2,-}(\pi/2 + n\pi)$  of Eqs. (43) and (44) is smaller than the coefficient “ $1/2$ ” of  $c_{x^2-y^2,-}^{x^2-y^2,-}(n\pi)$  in  $P_-^{x^2-y^2,-}(n\pi)$ . This relation reflects that  $|c_{3z^2-r^2,-}^{3z^2-r^2,-}(\pi/2 + n\pi)| \sim 1$  does not hold because of large hybridization at  $\theta = \pi/2 + n\pi$  between the degenerate  $d\gamma$  states through the  $d\varepsilon$  states, and then,  $|c_{x^2-y^2,-}^{3z^2-r^2,-}(\pi/2 + n\pi)|$  has non-negligible magnitude [also see  $\langle 3z^2 - r^2, \chi_-(\pi/2 + n\pi) | \mathcal{H} | xz, \chi_-(\pi/2 + n\pi) \rangle = i(\sqrt{3}\lambda/2)(-1)^n$  and  $\langle x^2 - y^2, \chi_-(\pi/2 + n\pi) | \mathcal{H} | xz, \chi_-(\pi/2 + n\pi) \rangle = -i(\lambda/2)(-1)^n$ ]. In contrast,  $|c_{x^2-y^2,-}^{x^2-y^2,-}(n\pi)| \sim 1$  is realized by the small hybridization at  $\theta = n\pi$  between the  $d\gamma$  states through the  $d\varepsilon$  states, as found from the fact that most of  $\langle j_1, \chi_-(n\pi) | \mathcal{H} | j_2, \chi_-(n\pi) \rangle$  are zero, where  $j_1 = x^2 - y^2$  or  $3z^2 - r^2$ , and  $j_2 = xy, yz$ , or  $xz$ .

### 4.2.3 Crystal field of tetragonal symmetry

We consider the system with the crystal field of tetragonal symmetry. In Fig. 3, we show the  $D_{\varepsilon,-}^{(d)}/D_{\gamma,-}^{(d)}$  ( $= r_{s,\sigma\rightarrow\varepsilon,-}/r_{s,\sigma\rightarrow\gamma,-}$ ) dependence of  $C_2$  of Eq. (41) [ $C_4$  of Eq. (42)] for the system with  $r_{s,+ \rightarrow \gamma 1,-} = r_{s,- \rightarrow \gamma 1,-} = 0.01$  by the solid red [dashed red] curve. We find that the system shows  $C_2 > 0$  and  $C_4 > 0$  for  $D_{\varepsilon,-}^{(d)}/D_{\gamma,-}^{(d)} < 1$ ,  $C_2 = C_4 = 0$  at  $D_{\varepsilon,-}^{(d)}/D_{\gamma,-}^{(d)} = 1$ , and  $C_2 < 0$  and  $C_4 < 0$  for  $D_{\varepsilon,-}^{(d)}/D_{\gamma,-}^{(d)} > 1$ . By using Eq. (38), TAMR( $\theta$ ) of Eq. (3) is then rewritten as

$$\text{TAMR}(\theta) = C_2(-1 + \cos 2\theta) + C_4(-1 + \cos 4\theta). \quad (68)$$

The system therefore exhibits the twofold and fourfold symmetric TAMR effect with  $\text{TAMR}(\theta) \leq 0$  for  $D_{\varepsilon,-}^{(d)}/D_{\gamma,-}^{(d)} < 1$  and  $\text{TAMR}(\theta) \geq 0$  for  $D_{\varepsilon,-}^{(d)}/D_{\gamma,-}^{(d)} > 1$ , while the system has  $\text{TAMR}(\theta) = 0$  at  $D_{\varepsilon,-}^{(d)}/D_{\gamma,-}^{(d)} = 1$ .

In Fig. 5(a), we show the  $\theta$  dependence of TAMR( $\theta$ ) of Eq. (2) for the  $d\varepsilon$ ,  $d\gamma$ , and  $d\varepsilon + d\gamma$  models. The curves represent results calculated directly by using the exact diagonalization method. The dots show the results obtained by substituting the evaluated  $C_2$ s of Eq. (41) and  $C_4$ s of Eq. (42) into TAMR( $\theta$ ) of Eq. (68), where  $C_2$  and  $C_4$  for each model are given in Table III. We find contradictory behavior of TAMR( $\theta$ ) between the  $d\varepsilon$  model and the  $d\gamma$  model. Namely, the  $d\varepsilon$  model exhibits  $\text{TAMR}(\theta) \geq 0$  and has two small peaks on a broad peak in one period (i.e.,  $0 \leq \theta < \pi$ ). Specifically, the  $d\varepsilon$  model takes the highest value 0.40 at  $\theta \sim \pi/4 + n\pi/2$  (Ref. 35) and the lowest value 0 at  $\theta = n\pi$ , where  $n = 0, \pm 1, \pm 2, \dots$ . In contrast, the  $d\gamma$  model shows  $\text{TAMR}(\theta) \leq 0$  and has two small dips in a broad dip in one period (i.e.,  $0 \leq \theta < \pi$ ). Specifically, the  $d\gamma$  model has the highest value 0 at  $\theta = n\pi$  and the lowest value  $-0.083$  at  $\theta \sim \pi/4 + n\pi/2$  (Ref. 35), where  $n = 0, \pm 1, \pm 2, \dots$ . The  $d\varepsilon + d\gamma$  model takes TAMR( $\theta$ ) between TAMR( $\theta$ ) of the  $d\varepsilon$  model and that of the  $d\gamma$  model. Namely, the  $d\varepsilon + d\gamma$  model has  $0 \leq \text{TAMR}(\theta) \leq 0.036$  for  $D_{\varepsilon,-}^{(d)}/D_{\gamma,-}^{(d)} = 1.5$ ,  $\text{TAMR}(\theta) = 0$  at  $D_{\varepsilon,-}^{(d)}/D_{\gamma,-}^{(d)} = 1$ , and  $-0.039 \leq \text{TAMR}(\theta) \leq 0$  for  $D_{\varepsilon,-}^{(d)}/D_{\gamma,-}^{(d)} = 0.5$ . In other words, the positive and large TAMR( $\theta$ ) for the  $d\varepsilon$  model is reduced by the negative TAMR( $\theta$ ) for the  $d\gamma$  model [see Eq. (B·5)].

We can explain the behavior of TAMR( $\theta$ ) in the same way as for the cubic system. First, the  $\theta$  dependences of TAMR( $\theta$ ) for the  $d\varepsilon$  and  $d\gamma$  models directly reflect those of  $P_-^{d\varepsilon,-}(\theta)$  and  $P_-^{d\gamma,-}(\theta)$ , respectively, as found from Eqs. (A·1)–(A·3), (B·1), and (B·2). In Fig. 5(b) [(c)], we show the  $\theta$  dependence of  $P_-^{d\varepsilon,-}(\theta)$  [ $P_-^{d\gamma,-}(\theta)$ ] by the black curve. In addition, Fig. 5(d) shows the  $\theta$  dependence of  $P_-^{d\varepsilon,-}(\theta) + P_-^{d\gamma,-}(\theta)$ . We find contradictory

**Table III.** The coefficients  $C_2$  of Eq. (41) and  $C_4$  of Eq. (42) for strong ferromagnets with a crystal field of tetragonal symmetry. The system has  $D_{j,+}^{(d)} = 0$  (i.e.,  $r_{s,\sigma \rightarrow j,+} = 0$ ),  $r = 0.001$ ,  $H = 1$  eV,  $\lambda = \lambda' = 0.05$  eV,  $\Delta = 0.1$  eV, and  $\delta = 0.05$  eV. For these systems, we consider  $d\varepsilon$ ,  $d\gamma$ , and  $d\varepsilon + d\gamma$  models. In particular, the  $d\varepsilon + d\gamma$  model has  $D_{\varepsilon,-}^{(d)}/D_{\gamma,-}^{(d)} = 0.5, 1$ , and  $1.5$ . Additionally, TAMR( $\theta$ ) of Eq. (68) with each set of  $C_2$  and  $C_4$  in this table is indicated by the dots in Fig. 5(a).

Model	$C_2$	$C_4$
$d\varepsilon$	-0.16	-0.11
$d\gamma$	0.033	0.022
$d\varepsilon + d\gamma$ ( $D_{\varepsilon,-}^{(d)}/D_{\gamma,-}^{(d)} = 0.5$ )	0.016	0.011
$d\varepsilon + d\gamma$ ( $D_{\varepsilon,-}^{(d)}/D_{\gamma,-}^{(d)} = 1$ )	0	0
$d\varepsilon + d\gamma$ ( $D_{\varepsilon,-}^{(d)}/D_{\gamma,-}^{(d)} = 1.5$ )	-0.014	-0.0096

behavior between  $P_-^{d\varepsilon,-}(\theta)$  and  $P_-^{d\gamma,-}(\theta)$ , in which  $P_-^{d\gamma,-}(\theta)$  decreases (increases) as  $P_-^{d\varepsilon,-}(\theta)$  increases (decreases). This behavior arises under the condition of  $P_-^{d\varepsilon,-}(\theta) + P_-^{d\gamma,-}(\theta) \approx 1/3$  of Eq. (C.2). The condition can be confirmed in Fig. 5(d). Next, we look at the value of TAMR( $\theta$ ) for the  $d\varepsilon + d\gamma$  model on the basis of the approximate expression of TAMR( $\theta$ ) of Eqs. (B.1)–(B.5). As seen from Eq. (B.8), TAMR( $\theta$ ) of Eq. (B.5) is less than or equal to that for the  $d\varepsilon$  model of Eq. (B.1) and greater than or equal to that for the  $d\gamma$  model of Eq. (B.2). In particular, when  $D_{\varepsilon,-}^{(d)}/D_{\gamma,-}^{(d)} = 1$ , TAMR( $\theta$ ) of Eq. (B.3) or (B.4) is 0 [see Eq. (B.9)].

We describe the details of  $P_-^{d\varepsilon,-}(\theta)$  of Eq. (64) for the  $d\varepsilon$  model [see Fig. 5(b)]. The quantity  $P_-^{d\varepsilon,-}(\theta)$  has peaks at  $\theta \sim \pi/4 + n\pi/2$  like the cubic system, where  $n = 0, \pm 1, \pm 2, \dots$ . The peaks come from  $P_-^{xy,-}(\theta)$ ,  $P_-^{yz,-}(\theta)$ , and  $P_-^{xz,-}(\theta)$  at  $\theta \sim \pi/4 + n\pi/2$ . Namely, the  $d\varepsilon$  states consisting of  $|xy, \chi_-(\theta)\rangle$ ,  $|yz, \chi_-(\theta)\rangle$ , and  $|xz, \chi_-(\theta)\rangle$  are strongly hybridized to the  $d\gamma_{x,-}$  states at  $\theta \sim \pi/4 + n\pi/2$ . In addition,  $P_-^{d\varepsilon,-}(n\pi)$  [ $P_-^{d\varepsilon,-}(\pi/2 + n\pi)$ ] is formed by only  $P_-^{xy,-}(n\pi)$  [ $P_-^{xz,-}(\pi/2 + n\pi)$ ] like the cubic system, where  $n = 0, \pm 1, \pm 2, \dots$ . We note, however, that the tetragonal system shows  $P_-^{xz,-}(\pi/2 + n\pi) > P_-^{xy,-}(n\pi)$ , whereas the cubic system has  $P_-^{xz,-}(\pi/2 + n\pi) = P_-^{xy,-}(n\pi)$  [see Fig. 4(b)]. The relation  $P_-^{xz,-}(\pi/2 + n\pi) > P_-^{xy,-}(n\pi)$  indicates that  $|xz, \chi_-(\theta)\rangle$  is strongly hybridized to the  $d\gamma_{x,-}$  states compared with  $|xy, \chi_-(\theta)\rangle$ , because the energy differences between  $|xz, \chi_-(\theta)\rangle$  and  $d\gamma$  states are smaller than those between  $|xy, \chi_-(\theta)\rangle$  and  $d\gamma$  states, as shown in Fig. 2. We also find  $P_-^{xy,-}(n\pi) > P_-^{yz,-}(\pi/4 + n\pi/2)$  like the cubic system. This relation means that the probability density of the  $d\gamma_{x,-}$  states in  $|xy, \chi_-(n\pi)\rangle$  is larger than that in  $|yz, \chi_-(\pi/4 + n\pi/2)\rangle$ .

We give the details of  $P_-^{d\gamma,-}(\theta)$  of Eq. (65) for the  $d\gamma$  model [see Fig. 5(c)]. The behavior of  $P_-^{d\gamma,-}(\theta)$  mainly comes from that of  $P_-^{x^2-y^2,-}(\theta)$  because of  $P_-^{x^2-y^2,-}(\theta) > P_-^{3z^2-r^2,-}(\theta)$  for the whole range of  $\theta$ . This feature is different from that for the cubic system. Namely,  $P_-^{x^2-y^2,-}(\theta) > P_-^{3z^2-r^2,-}(\theta)$  for the whole range of  $\theta$  does not correspond to  $P_-^{x^2-y^2,-}(n\pi) = P_-^{3z^2-r^2,-}(\pi/2+n\pi)$  for the cubic system. The relation  $P_-^{x^2-y^2,-}(\theta) > P_-^{3z^2-r^2,-}(\theta)$  shows that the probability density of  $|x^2 - y^2, \chi_-(\theta)\rangle$  of the  $x$  direction is always larger than that of  $|3z^2 - r^2, \chi_-(\theta)\rangle$  of the  $x$  direction. Roughly speaking,  $P_\sigma^{j,\zeta}(\theta)$  of Eq. (43) is approximately expressed as  $P_-^{x^2-y^2,-}(\theta) \approx (1/4) \left| c_{x^2-y^2,-}^{x^2-y^2,-}(\theta) \right|^2 \sim 1/4$  and  $P_-^{3z^2-r^2,-}(\theta) \approx (1/12) \left| c_{3z^2-r^2,-}^{3z^2-r^2,-}(\theta) \right|^2 \sim 1/12$  under the assumption of  $|c_{3z^2-r^2,-}^{x^2-y^2,-}(\theta)| \ll |c_{x^2-y^2,-}^{x^2-y^2,-}(\theta)| \sim 1$  and  $|c_{x^2-y^2,-}^{3z^2-r^2,-}(\theta)| \ll |c_{3z^2-r^2,-}^{3z^2-r^2,-}(\theta)| \sim 1$ , as found from the values of  $P_-^{x^2-y^2,-}(\theta)$  and  $P_-^{3z^2-r^2,-}(\theta)$  in Fig. 5(c). This assumption may be valid for the tetragonal system with small hybridization between nondegenerate  $d\gamma$  states (also see the submatrix of the  $d\gamma$  states in  $\mathcal{H}$  of Table I). We also find that  $P_-^{d\gamma,-}(\theta)$  has peaks at  $\theta = n\pi$ , with  $n = 0, \pm 1, \pm 2, \dots$ . The peaks originate from those of  $P_-^{x^2-y^2,-}(n\pi)$ . Here,  $|\psi_{x^2-y^2,-}(\theta)\rangle$  includes the  $d\gamma_{x,-}$  states with the highest probability density at  $\theta = n\pi$ .

## 5. Comment

On the basis of the above-mentioned results, we offer a comment on the experimental results of the temperature,  $T$ , dependences of  $C_2$  and  $C_4$  in TAMR( $\theta$ ) of Eq. (2) for Fe<sub>4</sub>N.<sup>21)</sup> Here, Fe<sub>4</sub>N is considered to be a strong ferromagnet.<sup>12,14,23)</sup> In addition, the parameters in Sect. 4 are appropriate for Fe<sub>4</sub>N.<sup>32)</sup>

The noteworthy experimental result is the enhancement of  $|C_2|$  and  $|C_4|$  with a decrease in temperature for  $T \lesssim 35$  K, i.e., (i)  $C_2 = 0$  and  $C_4 = -0.005$  at  $T \sim 35$  K and (ii)  $C_2 = -0.02$  and  $C_4 = -0.01$  at  $T = 5$  K.<sup>21)</sup> Result (i) agrees fairly well with  $C_2 = 0$  and  $C_4 = -0.0048$  evaluated for the  $d\varepsilon + d\gamma$  model of  $D_{\varepsilon,-}^{(d)}/D_{\gamma,-}^{(d)} = 1.5$  with a crystal field of ‘‘cubic’’ symmetry (see Table II). In contrast, result (ii) corresponds well with  $C_2 = -0.014$  and  $C_4 = -0.0096$  evaluated for the  $d\varepsilon + d\gamma$  model of  $D_{\varepsilon,-}^{(d)}/D_{\gamma,-}^{(d)} = 1.5$  with a crystal field of ‘‘tetragonal’’ symmetry (see Table III). Note here that this  $D_{\varepsilon,-}^{(d)}/D_{\gamma,-}^{(d)}$  (=1.5) is comparable to  $1.1 \lesssim D_{\varepsilon,-}^{(d)}/D_{\gamma,-}^{(d)} \lesssim 1.4$  evaluated from our theoretical analysis of the experimental result of the in-plane AMR effect for  $T \leq 35$  K (see Fig. 11 of Erratum II in Ref. 14). From the above result, we predict that the tetragonal distortion may proceed with decreasing temperature for  $T \lesssim 35$  K.

The tetragonal distortion has already been predicted also in our analysis of the experimental results of the in-plane AMR ratio for Fe<sub>4</sub>N,<sup>14)</sup> where the experimental

results show the appearance of  $C_4$  for  $T \leq 35$  K.<sup>7)</sup> Concretely, by using the electron scattering theory based on the second-order perturbation theory, we showed that a model with a crystal field of tetragonal symmetry can reproduce the appearance of  $C_4$ .<sup>14)</sup>

On the other hand, Yahagi *et al.* investigated the fourfold symmetric AMR effect for a cubic single-crystal ferromagnetic model by using the Kubo formula and the multi-orbital d-impurity Anderson model, where the d states have the spin-orbit interaction and crystal field of cubic symmetry.<sup>24)</sup> They found that  $C_4$  in the in-plane AMR ratio appears even for the cubic system as a result of the fourth-order perturbation with respect to the spin-orbit interaction. Here, the splitting of the d states due to the spin-orbit interaction is responsible for the appearance of  $C_4$ . Furthermore, by performing the numerical (i.e., nonperturbative) calculation for TAMR( $\theta$ ) of the cubic system, they showed that  $C_4$  appears by the same mechanism as the above-mentioned  $C_4$  in the in-plane AMR ratio. Simultaneously, they confirmed the absence of  $C_2$  in TAMR( $\theta$ ). The absence of  $C_2$  is certainly valid from the viewpoint of the symmetry of the cubic crystal. In addition, the absence of  $C_2$  for the cubic system is confirmed also in our present study based on the exact diagonalization method (see Sect. 4.2.2).

We emphasize, however, that the experimental result of TAMR( $\theta$ ) for Fe<sub>4</sub>N shows  $C_2 \neq 0$  for  $T \lesssim 35$  K.<sup>21)</sup> This  $C_2 \neq 0$  is actually obtained for the tetragonal system with the finite  $\delta$  of Eq. (66) in our present study (see Sect. 4.2.3). Therefore, we guess that the tetragonal distortion may be necessary to explain the experimental results of both TAMR( $\theta$ ) and the in-plane AMR ratio for Fe<sub>4</sub>N.

## 6. Conclusion

We developed a theory of the anisotropic magnetoresistance effects of arbitrary directions of  $\mathbf{I}$  and  $\mathbf{M}$  for ferromagnets. Here, we used the electron scattering theory with  $s$ - $d$  scattering processes. The  $s$ - $d$  scattering means that the conduction electron is scattered into the localized d states by a nonmagnetic impurity. The resistivity due to the  $s$ - $d$  scattering directly reflects the probability density of the d states of the  $\mathbf{I}$  direction. The d states are numerically obtained by applying the exact diagonalization method to the Hamiltonian of the d states with the exchange field, crystal field, and spin-orbit interaction. Using this theory, we investigated the TAMR effect for strong ferromagnets with a crystal field of cubic or tetragonal symmetry. The cubic system exhibits the fourfold TAMR effect, whereas the tetragonal system shows the twofold and

fourfold TAMR effect. In addition, the cubic or tetragonal system has  $\text{TAMR}(\theta) \leq 0$  for  $D_{\varepsilon,-}^{(d)}/D_{\gamma,-}^{(d)} < 1$ ,  $\text{TAMR}(\theta) = 0$  at  $D_{\varepsilon,-}^{(d)}/D_{\gamma,-}^{(d)} = 1$ , and  $\text{TAMR}(\theta) \geq 0$  for  $D_{\varepsilon,-}^{(d)}/D_{\gamma,-}^{(d)} > 1$ . We also found contradictory behavior of  $\text{TAMR}(\theta)$  between the  $d\varepsilon$  model with  $D_{\varepsilon,-}^{(d)} \neq 0$  and  $D_{\gamma,-}^{(d)} = 0$  and the  $d\gamma$  model with  $D_{\varepsilon,-}^{(d)} = 0$  and  $D_{\gamma,-}^{(d)} \neq 0$ . Such behavior appears under the condition for the probability density of the d states of the  $\mathbf{I}$  direction. Finally, on the basis of the calculation results, we commented on the experimental results of the TAMR effect for  $\text{Fe}_4\text{N}$ , i.e., the enhancement of  $|C_2|$  and  $|C_4|$  with a decrease in temperature. We predicted that the tetragonal distortion may proceed with decreasing temperature.

### Acknowledgments

We would like to thank Mr. Yuta Yahagi of Tohoku University for useful discussion. This work has been supported by the Cooperative Research Project (H31/A06) of the RIEC, Tohoku University, and Grants-in-Aid for Scientific Research (C) (No. 19K05249) and (B) (No. 20H02177) from the Japan Society for the Promotion of Science.

### Appendix A: TAMR( $\theta$ ) and $P_{\sigma}^{j,s}(\theta)$

We describe the relations between  $\text{TAMR}(\theta)$  and  $P_{\sigma}^{j,s}(\theta)$  for the  $d\varepsilon$ ,  $d\gamma$ , and  $d\varepsilon + d\gamma$  models of a strong ferromagnet with  $D_{j,+}^{(d)} = 0$ ,  $\sum_j D_{j,-}^{(d)} \neq 0$ ,  $r \ll 1$ , and  $r_{s,\sigma \rightarrow j,-} \ll 1$ , where the actual parameters are given in Sect. 4.1. To begin with, we simply write  $\text{TAMR}(\theta)$  of Eq. (2) for this system as

$$\text{TAMR}(\theta) \approx \frac{\rho_-(\theta) - \rho_-(0)}{\rho_-(0)}. \quad (\text{A}\cdot 1)$$

Here, we have used

$$\rho(\theta) = \frac{\rho_+(\theta)\rho_-(\theta)}{\rho_+(\theta) + \rho_-(\theta)} = \frac{\rho_+(\theta)\rho_-(\theta)}{\rho_+(\theta)[1 + \rho_-(\theta)/\rho_+(\theta)]} \approx \rho_-(\theta), \quad (\text{A}\cdot 2)$$

which is obtained on the basis of  $\rho_-(\theta)/\rho_+(\theta) \ll 1$ .<sup>36)</sup> The angle  $\theta$  dependence of  $\text{TAMR}(\theta)$  of Eq. (A.1) thus reflects that of  $\rho_-(\theta)$ . The angle  $\theta$  dependence of  $\rho_-(\theta)$  results from that of  $\sum_j \sum_{\varsigma} 1/\tau_{s,-\rightarrow j,\varsigma}(\theta)$  of Eqs. (25) and (36) [also see Eqs. (19) and (20)]. We now substitute  $D_{j,+}^{(d)} = 0$  into  $\sum_j \sum_{\varsigma} 1/\tau_{s,-\rightarrow j,\varsigma}(\theta)$ . In addition, we take into account  $D_{\varepsilon,-}^{(d)} \neq 0$  and  $D_{\gamma,-}^{(d)} = 0$  for the  $d\varepsilon$  model,  $D_{\varepsilon,-}^{(d)} = 0$  and  $D_{\gamma,-}^{(d)} \neq 0$  for the  $d\gamma$  model, and  $D_{\varepsilon,-}^{(d)} \neq 0$  and  $D_{\gamma,-}^{(d)} \neq 0$  for the  $d\varepsilon + d\gamma$  model. As a result, we can express  $\sum_j \sum_{\varsigma} 1/\tau_{s,-\rightarrow j,\varsigma}(\theta)$  of Eqs. (25) and (36) as

$$\sum_j \sum_{\varsigma} \frac{1}{\tau_{s,-\rightarrow j,\varsigma}(\theta)} = \frac{2\pi}{\hbar} n_{\text{imp}} N_{\text{n}} v_{\text{n}}^2 \sum_j P_{-}^{j,-}(\theta) D_{j,-}^{(d)}$$

$$= \begin{cases} \frac{2\pi}{\hbar} n_{\text{imp}} N_n v_-^2 P_-^{d\varepsilon,-}(\theta) D_{\varepsilon,-}^{(d)}, & \text{for } d\varepsilon \text{ model,} \\ \frac{2\pi}{\hbar} n_{\text{imp}} N_n v_-^2 P_-^{d\gamma,-}(\theta) D_{\gamma,-}^{(d)}, & \text{for } d\gamma \text{ model,} \\ \frac{2\pi}{\hbar} n_{\text{imp}} N_n v_-^2 \left[ P_-^{d\varepsilon,-}(\theta) D_{\varepsilon,-}^{(d)} + P_-^{d\gamma,-}(\theta) D_{\gamma,-}^{(d)} \right], & \text{for } d\varepsilon + d\gamma \text{ model,} \end{cases} \quad (\text{A}\cdot 3)$$

where  $P_-^{d\varepsilon,-}(\theta)$  [ $P_-^{d\gamma,-}(\theta)$ ] is given by Eq. (64) [(65)], and  $D_{\varepsilon,-}^{(d)}$  [ $D_{\gamma,-}^{(d)}$ ] is given by Eq. (60) [(61)].

### Appendix B: TAMR( $\theta$ ) for $d\varepsilon$ , $d\gamma$ , and $d\varepsilon + d\gamma$ models

Using Eqs. (A.1), (A.3), (46)–(50), (19), and (20), we obtain the approximate expression of TAMR( $\theta$ ) for the  $d\varepsilon$ ,  $d\gamma$ , and  $d\varepsilon + d\gamma$  models of a strong ferromagnet. The expression of TAMR( $\theta$ ) for the  $d\varepsilon$  model is given by

$$\text{TAMR}(\theta) = \frac{3 \left[ P_-^{d\varepsilon,-}(\theta) - P_-^{d\varepsilon,-}(0) \right] r_{s,-\rightarrow\varepsilon,-}}{r + 3P_-^{d\varepsilon,-}(0)r_{s,-\rightarrow\varepsilon,-}} \equiv \text{TAMR}_{d\varepsilon}(\theta). \quad (\text{B}\cdot 1)$$

The expression of TAMR( $\theta$ ) for the  $d\gamma$  model is

$$\text{TAMR}(\theta) = \frac{3 \left[ P_-^{d\gamma,-}(\theta) - P_-^{d\gamma,-}(0) \right] r_{s,-\rightarrow\gamma,-}}{r + 3P_-^{d\gamma,-}(0)r_{s,-\rightarrow\gamma,-}} \equiv \text{TAMR}_{d\gamma}(\theta). \quad (\text{B}\cdot 2)$$

The expression of TAMR( $\theta$ ) for the  $d\varepsilon + d\gamma$  model is

$$\text{TAMR}(\theta) = \frac{3 \left[ P_-^{d\varepsilon,-}(\theta) - P_-^{d\varepsilon,-}(0) \right] (r_{s,-\rightarrow\varepsilon,-} - r_{s,-\rightarrow\gamma,-})}{r + 3P_-^{d\varepsilon,-}(0)r_{s,-\rightarrow\varepsilon,-} + \left[ 1 - 3P_-^{d\varepsilon,-}(0) \right] r_{s,-\rightarrow\gamma,-}} \equiv \text{TAMR}_{d\varepsilon+d\gamma}(\theta), \quad (\text{B}\cdot 3)$$

or

$$\text{TAMR}(\theta) = \frac{3 \left[ P_-^{d\gamma,-}(\theta) - P_-^{d\gamma,-}(0) \right] (r_{s,-\rightarrow\gamma,-} - r_{s,-\rightarrow\varepsilon,-})}{r + 3P_-^{d\gamma,-}(0)r_{s,-\rightarrow\gamma,-} + \left[ 1 - 3P_-^{d\gamma,-}(0) \right] r_{s,-\rightarrow\varepsilon,-}} \equiv \text{TAMR}_{d\varepsilon+d\gamma}(\theta), \quad (\text{B}\cdot 4)$$

where the condition of Eq. (C.2) has been used. This TAMR( $\theta$ ) of Eq. (B.3) or (B.4) can be rewritten as

$$\text{TAMR}(\theta) = (1 - X)\text{TAMR}_{d\varepsilon}(\theta) + (1 - Y)\text{TAMR}_{d\gamma}(\theta) \equiv \text{TAMR}_{d\varepsilon+d\gamma}(\theta), \quad (\text{B}\cdot 5)$$

with

$$X = \frac{\left[ 1 - 3P_-^{d\varepsilon,-}(0) \right] r_{s,-\rightarrow\gamma,-}}{r + 3P_-^{d\varepsilon,-}(0)r_{s,-\rightarrow\varepsilon,-} + \left[ 1 - 3P_-^{d\varepsilon,-}(0) \right] r_{s,-\rightarrow\gamma,-}}, \quad (\text{B}\cdot 6)$$

$$Y = \frac{\left[1 - 3P_-^{d\gamma,-}(0)\right] r_{s,-\rightarrow\varepsilon,-}}{r + 3P_-^{d\gamma,-}(0)r_{s,-\rightarrow\gamma,-} + \left[1 - 3P_-^{d\gamma,-}(0)\right] r_{s,-\rightarrow\varepsilon,-}}, \quad (\text{B}\cdot 7)$$

where  $0 \lesssim X < 1$  and  $0 \lesssim Y < 1$ . The range of  $X$  [ $Y$ ] is given by using  $1 - 3P_-^{d\varepsilon,-}(0) \gtrsim 0$  [ $1 - 3P_-^{d\gamma,-}(0) \gtrsim 0$ ] obtained from the condition of Eq. (C·2). Here, when  $r_{s,-\rightarrow\gamma,-} = 0$  [i.e.,  $D_{\gamma,-}^{(d)} = 0$ ],  $\text{TAMR}_{d\varepsilon+d\gamma}(\theta)$  of Eq. (B·5) reduces to  $\text{TAMR}_{d\varepsilon}(\theta)$  of Eq. (B·1). When  $r_{s,-\rightarrow\varepsilon,-} = 0$  [i.e.,  $D_{\varepsilon,-}^{(d)} = 0$ ],  $\text{TAMR}_{d\varepsilon+d\gamma}(\theta)$  of Eq. (B·5) becomes  $\text{TAMR}_{d\gamma}(\theta)$  of Eq. (B·2). In addition,  $\text{TAMR}_{d\varepsilon+d\gamma}(\theta)$  approaches  $\text{TAMR}_{d\varepsilon}(\theta)$  with increasing  $r_{s,-\rightarrow\varepsilon,-}/r_{s,-\rightarrow\gamma,-}$  [i.e.,  $D_{\varepsilon,-}^{(d)}/D_{\gamma,-}^{(d)}$ ], while  $\text{TAMR}_{d\varepsilon+d\gamma}(\theta)$  approaches  $\text{TAMR}_{d\gamma}(\theta)$  with decreasing  $r_{s,-\rightarrow\varepsilon,-}/r_{s,-\rightarrow\gamma,-}$ . In the case of  $\text{TAMR}_{d\varepsilon}(\theta) \geq 0$  and  $\text{TAMR}_{d\gamma}(\theta) \leq 0$  shown in Figs. 4(a) and 5(a), we obtain the following relation from Eq. (B·5):

$$\text{TAMR}_{d\gamma}(\theta) \leq \text{TAMR}_{d\varepsilon+d\gamma}(\theta) \leq \text{TAMR}_{d\varepsilon}(\theta), \quad (\text{B}\cdot 8)$$

regardless of  $r_{s,-\rightarrow\varepsilon,-}/r_{s,-\rightarrow\gamma,-}$  [i.e.,  $D_{\varepsilon,-}^{(d)}/D_{\gamma,-}^{(d)}$ ]. From Eq. (B·3) or (B·4), we also have

$$\text{TAMR}_{d\varepsilon+d\gamma}(\theta) = 0, \quad (\text{B}\cdot 9)$$

for  $r_{s,-\rightarrow\varepsilon,-} = r_{s,-\rightarrow\gamma,-}$  [i.e.,  $D_{\varepsilon,-}^{(d)} = D_{\gamma,-}^{(d)}$ ]. Equations (B·8) and (B·9) are utilized in Sects. 4.2.2 and 4.2.3 [also see Figs. 4(a) and 5(a)].

### Appendix C: Condition for $P_-^{d\varepsilon,-}(\theta) + P_-^{d\gamma,-}(\theta)$

On the basis of the condition of  $\sum_j \sum_\varsigma P_\sigma^{j,\varsigma}(\theta) = 1/3$  of Eq. (45), we derive the condition for  $P_-^{d\varepsilon,-}(\theta) + P_-^{d\gamma,-}(\theta)$  [see Eqs. (64), (65), and (43)]. We now focus on  $c_{i,\sigma}^{j,\varsigma}(\theta)$  in  $|\psi_{j,\varsigma}(\theta)\rangle$  of Eqs. (13) and (33) under the present parameters with  $\lambda/H \ll \lambda/\Delta < 1$  for the cubic system or  $\lambda/H \ll \lambda/\Delta < \lambda/\delta = 1$  for the tetragonal system, where the actual parameters are given in Sect. 4.1. Here, we have the relation  $|c_{i,-}^{j,+}(\theta)| \ll |c_{i,-}^{j,-}(\theta)|$  because mixing between the different spin states occurs between the states separated by the energy differences with  $H$ , while mixing between the same spin states occurs between the states separated by the energy differences with  $\Delta$  and/or  $\delta$  (see  $\mathcal{H}$  of Table I). From this relation and Eq. (43), we may then write the left-hand side of Eq. (45),  $\sum_j \sum_\varsigma P_-^{j,\varsigma}(\theta)$ , as

$$\sum_{\substack{j=xy,yz,xz \\ x^2-y^2, 3z^2-r^2}} \sum_{\varsigma=+,-} P_-^{j,\varsigma}(\theta) \approx \sum_{\substack{j=xy,yz,xz \\ x^2-y^2, 3z^2-r^2}} P_-^{j,-}(\theta). \quad (\text{C}\cdot 1)$$



Using Eqs. (45) and (C.1), we approximately obtain

$$\sum_{\substack{j=xy,yz,xz \\ x^2-y^2, 3z^2-r^2}} P_-^{j,-}(\theta) = P_-^{d\varepsilon,-}(\theta) + P_-^{d\gamma,-}(\theta) \approx \frac{1}{3}. \quad (\text{C}\cdot 2)$$

Equation (C.2) is the condition for  $P_-^{d\varepsilon,-}(\theta) + P_-^{d\gamma,-}(\theta)$ .

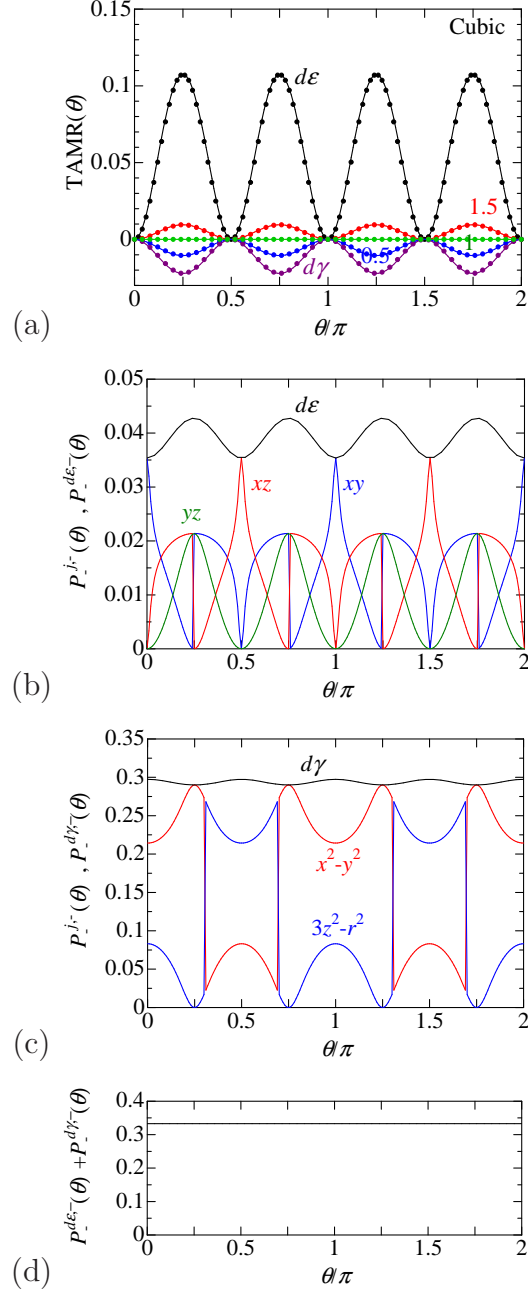


**Fig. 4.** (Color) The case of strong ferromagnets with a crystal field of cubic symmetry. The system has  $D_{j,+}^{(d)} = 0$  (i.e.,  $r_{s,\sigma \rightarrow j,+} = 0$ ),  $r = 0.001$ ,  $H = 1$  eV,  $\lambda = \lambda' = 0.05$  eV, and  $\Delta = 0.1$  eV. (a) The angle  $\theta$  dependences of TAMR( $\theta$ ) for the  $d\varepsilon$ ,  $d\gamma$ , and  $d\varepsilon + d\gamma$  models. The results for the  $d\varepsilon$  and  $d\gamma$  models are indicated by the black and purple curves, respectively. The results for the  $d\varepsilon + d\gamma$  model with  $D_{\varepsilon,-}^{(d)}/D_{\gamma,-}^{(d)} = 0.5, 1, \text{ and } 1.5$  are indicated by the blue, green, and red curves, respectively. In addition, the respective colored dots represent TAMR( $\theta$ ) of Eq. (67) with the evaluated  $C_4$ s of Eq. (42), where  $C_4$  for each model is given in Table II. (b) The angle  $\theta$  dependences of  $P_{-}^{d\varepsilon,-}(\theta)$ ,  $P_{-}^{xy,-}(\theta)$ ,  $P_{-}^{yz,-}(\theta)$ , and  $P_{-}^{xz,-}(\theta)$  for the  $d\varepsilon$  model. Here,  $P_{-}^{d\varepsilon,-}(\theta)$ ,  $P_{-}^{xy,-}(\theta)$ ,  $P_{-}^{yz,-}(\theta)$ , and  $P_{-}^{xz,-}(\theta)$  are indicated by the black, blue, green, and red curves, respectively. (c) The angle  $\theta$  dependences of  $P_{-}^{d\gamma,-}(\theta)$ ,  $P_{-}^{x^2-y^2,-}(\theta)$ , and  $P_{-}^{3z^2-r^2,-}(\theta)$  for the  $d\gamma$  model. Here,  $P_{-}^{d\gamma,-}(\theta)$ ,  $P_{-}^{x^2-y^2,-}(\theta)$ , and  $P_{-}^{3z^2-r^2,-}(\theta)$  are indicated by the black, red, and blue curves, respectively. (d) The angle  $\theta$  dependences of  $P_{-}^{d\varepsilon,-}(\theta) + P_{-}^{d\gamma,-}(\theta)$ . Here,  $P_{-}^{d\varepsilon,-}(\theta) + P_{-}^{d\gamma,-}(\theta)$  is the sum of  $P_{-}^{d\varepsilon,-}(\theta)$  in (b) and  $P_{-}^{d\gamma,-}(\theta)$  in (c).

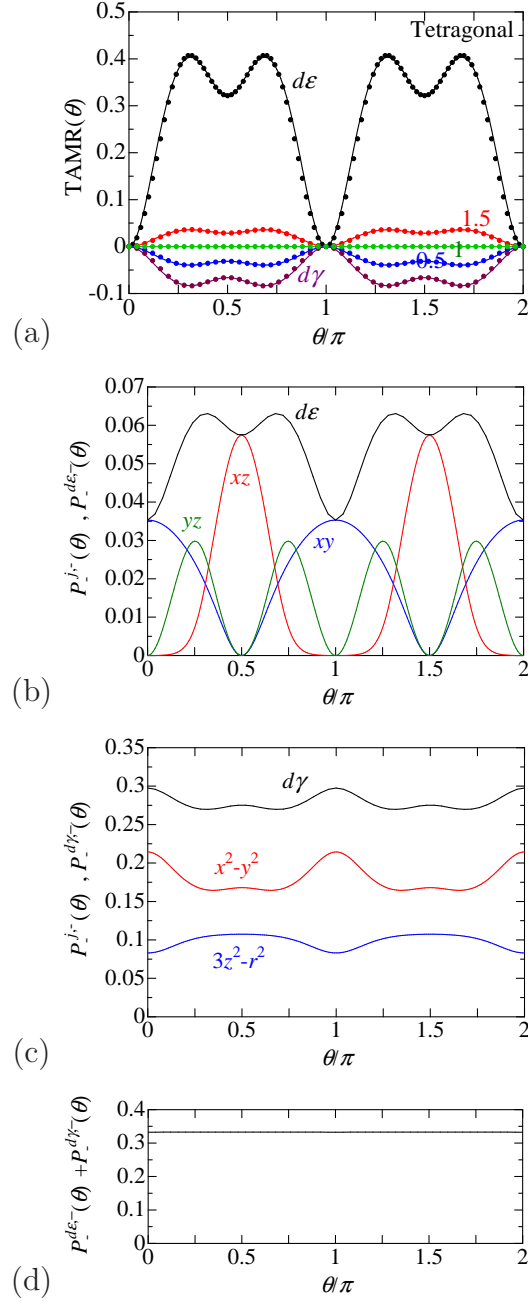


**Fig. 5.** (Color) The case of strong ferromagnets with a crystal field of tetragonal symmetry. The system has  $D_{j,+}^{(d)} = 0$  (i.e.,  $r_{s,\sigma \rightarrow j,+} = 0$ ),  $r = 0.001$ ,  $H = 1$  eV,  $\lambda = \lambda' = 0.05$  eV,  $\Delta = 0.1$  eV, and  $\delta = 0.05$  eV. The notation is the same as in Fig. 4. In (a), however, the respective colored dots show TAMR( $\theta$ ) of Eq. (68) with the evaluated  $C_2$ s of Eq. (41) and  $C_4$ s of Eq. (42), where  $C_2$  and  $C_4$  for each model are given in Table III. Furthermore,  $P_{-}^{d\varepsilon,-}(\theta) + P_{-}^{d\gamma,-}(\theta)$  in (d) is the sum of  $P_{-}^{d\varepsilon,-}(\theta)$  in (b) and  $P_{-}^{d\gamma,-}(\theta)$  in (c).

## References

- 1) W. Thomson, Proc. R. Soc. London **8**, 546 (1856).
- 2) T. R. McGuire, J. A. Aboaf, and E. Klokholm, IEEE Trans. Magn. **20**, 972 (1984).
- 3) I. A. Campbell, A. Fert, and O. Jaoul, J. Phys. C **3**, S95 (1970).
- 4) L. Berger, J. Appl. Phys. **67**, 5549 (1990).
- 5) T. Miyazaki and H. Jin, *The Physics of Ferromagnetism* (Springer Series, New York, 2012) Sect. 11.4.
- 6) M. Tsunoda, Y. Komasaki, S. Kokado, S. Isogami, C.-C. Chen, and M. Takahashi, Appl. Phys. Express **2**, 083001 (2009).
- 7) M. Tsunoda, H. Takahashi, S. Kokado, Y. Komasaki, A. Sakuma, and M. Takahashi, Appl. Phys. Express **3**, 113003 (2010).
- 8) K. Kabara, M. Tsunoda, and S. Kokado, Appl. Phys. Express **7**, 063003 (2014).
- 9) K. Kabara, M. Tsunoda, and S. Kokado, AIP Adv. **7**, 056416 (2017).
- 10) F. J. Yang, Y. Sakuraba, S. Kokado, Y. Kota, A. Sakuma, and K. Takanashi, Phys. Rev. B **86**, 020409 (2012).
- 11) Y. Sakuraba, S. Kokado, Y. Hirayama, T. Furubayashi, H. Sukegawa, S. Li, Y. K. Takahashi, and K. Hono, Appl. Phys. Lett. **104**, 172407 (2014).
- 12) S. Kokado, M. Tsunoda, K. Harigaya, and A. Sakuma, J. Phys. Soc. Jpn. **81**, 024705 (2012).
- 13) S. Kokado and M. Tsunoda, Adv. Mater. Res. **750–752**, 978 (2013).
- 14) S. Kokado and M. Tsunoda, J. Phys. Soc. Jpn. **84**, 094710 (2015). As Erratum I for this paper, see S. Kokado and M. Tsunoda, J. Phys. Soc. Jpn. **86**, 108001 (2017). As Erratum II for this paper, see S. Kokado and M. Tsunoda, J. Phys. Soc. Jpn. **88**, 068001 (2019).
- 15) S. Kokado, Y. Sakuraba, and M. Tsunoda, Jpn. J. Appl. Phys. **55**, 108004 (2016).
- 16) S. Kokado and M. Tsunoda, J. Phys. Soc. Jpn. **88**, 034706 (2019).
- 17) S. Kokado and M. Tsunoda, Mater. Today: Proc. **33**, 1864 (2020).
- 18) D. Zhao, S. Qiao, Y. Luo, A. Chen, P. Zhang, P. Zheng, Z. Sun, M. Guo, F.-K. Chiang, J. Wu, J. Luo, J. Li, S. Kokado, Y. Wang, and Y. Zhao, ACS Appl. Mater. Interfaces **9**, 10835 (2017).

- 19) T. Sato, S. Kokado, S. Kosaka, T. Ishikawa, T. Ogawa, and M. Tsunoda, *Appl. Phys. Lett.* **113**, 112407 (2018).
- 20) T. Sato, S. Kokado, M. Tsujikawa, T. Ogawa, S. Kosaka, M. Shirai, and M. Tsunoda, *Appl. Phys. Express* **12**, 103005 (2019).
- 21) K. Kabara, M. Tsunoda, and S. Kokado, *AIP Adv.* **6**, 055818 (2016).
- 22) M. Tsunoda, K. Kabara, and S. Kokado, *Magnetics Jpn.* **11**, 125 (2016) [in Japanese].
- 23) For a definition of a strong ferromagnet, see, for example, J. F. Janak, *Phys. Rev. B* **20**, 2206 (1979).
- 24) Y. Yahagi, D. Miura, and A. Sakuma, *J. Phys. Soc. Jpn.* **89**, 044714 (2020).
- 25) W. Zhou, T. Seki, T. Kubota, G. E. W. Bauer, and K. Takanashi, *Phys. Rev. Mater.* **2**, 094404 (2018).
- 26) H. Ibach and H. Lüth, *Solid-State Physics: An Introduction to Principles of Materials Science* (Springer, New York, 2009) 4th ed., Sect. 9.5. In particular, see Eq. (9.58a).
- 27) G. Grosso and G. P. Parravicini, *Solid State Physics* (Academic Press, New York, 2000) Chap. XI, Sect. 4.1.
- 28) In the calculation process from Eq. (21) to Eq. (25), we perform the integration with respect to  $\mathbf{r}$  in  $(\psi_{j,\varsigma}(\theta, \phi)|e^{i\mathbf{k}\cdot\mathbf{r}}, \chi_{\sigma}(\theta, \phi))$ . The result of the integration was given by Eq. (C.1) in Ref. 14.
- 29) K. Yosida, *Theory of Magnetism* (Springer Series, New York, 1998) Sect. 3.2.
- 30) The scattering rate  $1/\tau_{s,\sigma\rightarrow j,\varsigma}^{(0)}$  of Eq. (50) corresponds to  $1/\tau_{s,\sigma\rightarrow m,\varsigma}$  of Eq. (50) in Ref. 16.
- 31) In Sects. 2.5.1 and 3.1 in Ref. 12 and Sect. 3.1 in Ref. 14, we used a simple model with  $n_+ = n_-$ ,  $m_+^* = m_-^*$ , and  $v_+ = v_-$ , where  $v_+^2$  ( $v_-^2$ ) corresponds to  $3|V_{s\uparrow\rightarrow d\uparrow}|^2$  ( $3|V_{s\downarrow\rightarrow d\downarrow}|^2$ ) in Eq. (21) in Ref. 12. In Ref. 4, the author set  $n_+ = n_-$  and  $m_+^* = m_-^*$ , and ignored the  $\sigma$  dependence of parts corresponding to  $v_{\sigma}$ .
- 32) These parameters are close to those used in a theoretical analysis for Fe<sub>4</sub>N in Ref. 14. The parameters for Fe<sub>4</sub>N are  $H = 1$  eV,  $\lambda = \lambda' = 0.052$  eV,  $\Delta = 0.1$  eV,  $r = 0.0016$ , and  $r_{s,\sigma\rightarrow j,-} = 0.01$ , where  $r_{s,\sigma\rightarrow j,-}$  of Eq. (47) corresponds to  $r_{i,-}$  of Eq. (68) in Ref. 14. Here,  $r$  was evaluated from analyses using a combination of the first principles calculation and the Kubo formula (see Table I in Ref. 12). In addition,  $r_{s,\sigma\rightarrow j,-}$  was

evaluated to be  $0.01 \lesssim r_{s,\sigma \rightarrow j,-} \lesssim 0.5$  from theoretical analyses of the experimental result of the in-plane AMR ratio (see Sect. 3.3 in Ref. 12), where  $r_{s,\sigma \rightarrow j,-}$  of Eq. (47) corresponds to  $\rho_{s \rightarrow d\downarrow}/\rho_{s\uparrow}$  in Sect. 3.3 in Ref. 12.

33) In Ref. 12, we obtained  $\rho_{\perp,\sigma}$  of Eqs. (24) and (25) applying the perturbation theory to the ferromagnet with no crystal field. Here,  $\rho_{\perp,\sigma}$  is a resistivity of the  $\sigma$  spin for  $\mathbf{I} \perp \mathbf{M}$ . From the expression of  $\rho_{\perp,\sigma}$ , we find that  $\rho_{\perp,\sigma}$  is constant independent of the direction of  $\mathbf{M}$ , where  $\mathbf{M}$  is rotatable in a plane perpendicular to  $\mathbf{I}$ . The system therefore has  $\text{TAMR}(\theta) = 0$ .

34) The d orbital states are given by  $|xy\rangle = \frac{1}{\sqrt{2i}}(u_2 - u_{-2}) = xyf(r)$ ,  $|yz\rangle = -\frac{1}{\sqrt{2i}}(u_1 + u_{-1}) = yzf(r)$ ,  $|xz\rangle = -\frac{1}{\sqrt{2}}(u_1 - u_{-1}) = xzf(r)$ ,  $|x^2 - y^2\rangle = \frac{1}{\sqrt{2}}(u_2 + u_{-2}) = \frac{1}{2}(x^2 - y^2)f(r)$ , and  $|3z^2 - r^2\rangle = u_0 = \frac{1}{2\sqrt{3}}(3z^2 - r^2)f(r)$ . Here,  $u_m$  is the 3d orbital state with the magnetic quantum number  $m$ , where  $m = -2, -1, 0, 1, \text{ and } 2$ .

35) We can actually obtain the exact values of  $\theta$  that take the extreme values of  $\text{TAMR}(\theta)$  in Fig. 5. Here,  $\text{TAMR}(\theta)$  is expressed by Eq. (68), where the values of  $C_2$  and  $C_4$  are given in Table III. The values of  $\theta$  are obtained from  $\frac{d}{d\theta}\text{TAMR}(\theta) = 0$ . From  $\frac{d}{d\theta}\text{TAMR}(\theta) = -2 \sin 2\theta(C_2 + 4C_4 \cos 2\theta) = 0$ , we have  $\theta = \frac{1}{2} \sin^{-1} 0$  or  $\theta = \frac{1}{2} \cos^{-1} \left( -\frac{C_2}{4C_4} \right)$ . In the  $d\varepsilon$  model with  $C_2 = -0.16$  and  $C_4 = -0.11$ , the values of  $\theta$  are  $0, 0.31\pi, \pi/2, \text{ and } 0.69\pi$  for one period of  $0 \leq \theta < \pi$ . The other models in Table III also have the same  $\theta$  values as those above.

36) On the basis of our previous study,<sup>14,16,17)</sup> we confirm  $\rho_-(\theta)/\rho_+(\theta) \ll 1$  for the strong ferromagnet with  $D_{j,+}^{(d)} = 0$ ,  $\sum_j D_{j,-}^{(d)} \neq 0$ ,  $r \ll 1$ , and  $r_{s,\sigma \rightarrow j,-} \ll 1$  (see Sect. 4.1). Here, we have  $\lambda/H \ll \lambda/\Delta < 1$  for the cubic system and  $\lambda/H \ll \lambda/\Delta < \lambda/\delta = 1$  for the tetragonal system. We previously obtained the analytic expression of  $\rho_{\pm}(\theta)$  for the in-plane AMR effect within the second-order perturbation theory.<sup>14,16,17)</sup> On the basis of the previous study [e.g., Eq. (3) in Ref. 17], we infer that an expression of  $\rho_{\pm}(\theta)$  for the TAMR effect may be roughly expressed as  $\rho_{\pm}(\theta) = \rho_{s,\pm} + \rho_{s,\pm \rightarrow d,\pm} + [f_{1,\pm} + f_{2,\pm}(\theta)]\rho_{s,\pm \rightarrow d,\pm} + [g_{1,\pm} + g_{2,\pm}(\theta)]\rho_{s,\pm \rightarrow d,\mp}$ . Here,  $\rho_{s,\sigma \rightarrow d,-}$  corresponds to  $\rho_{s,\sigma \rightarrow j,-}$  of Eq. (49), and  $f_{1,\pm} + f_{2,\pm}(\theta)$  [ $g_{1,\pm} + g_{2,\pm}(\theta)$ ] represents the coefficient of the  $\rho_{s,\pm \rightarrow d,\pm}$  [ $\rho_{s,\pm \rightarrow d,\mp}$ ] term, where  $f_{1,\pm}$  and  $g_{1,\pm}$  are the terms independent of  $\theta$ , and  $f_{2,\pm}(\theta)$  and  $g_{2,\pm}(\theta)$  are the functions of  $\theta$ . In addition,  $|f_{1,\pm} + f_{2,\pm}(\theta)|$  and  $|g_{1,\pm} + g_{2,\pm}(\theta)|$  are considered to be at most 1 when  $\lambda/H \ll \lambda/\Delta < 1$  for the cubic system or  $\lambda/H \ll \lambda/\Delta < \lambda/\delta = 1$  for the tetragonal system (also

see  $\mathcal{H}$  of Table I). In the case of  $D_{j,+}^{(d)} = 0$  (i.e.,  $\rho_{s,\sigma \rightarrow j,+} = 0$ ), we have  $\rho_+(\theta) = \rho_{s,+} + [g_{1,+} + g_{2,+}(\theta)]\rho_{s,+ \rightarrow d,-}$  and  $\rho_-(\theta) = \rho_{s,-} + \rho_{s,- \rightarrow d,-} + [f_{1,-} + f_{2,-}(\theta)]\rho_{s,- \rightarrow d,-}$ . As a result, when  $r \ll 1$  and  $r_{s,\sigma \rightarrow j,-} \ll 1$  (i.e.,  $r_{s,\sigma \rightarrow d,-} \ll 1$ ), we obtain  $\rho_-(\theta)/\rho_+(\theta) = \{r + r_{s,- \rightarrow d,-} + [f_{1,-} + f_{2,-}(\theta)]r_{s,- \rightarrow d,-}\} / \{1 + [g_{1,+} + g_{2,+}(\theta)]r_{s,+ \rightarrow d,-}\} \ll 1$ , where  $r_{s,\sigma \rightarrow d,-} = \rho_{s,\sigma \rightarrow d,-} / \rho_{s,+}$ .